MSFC
MTP-TEST-MC-61-21
December 27, 1961

GEORGE C. MARSHALL SPACE FLIGHT CENTER
HUNTSVILLE, ALABAMA

ACOUSTIC FOCAL ZONES AROUND SATURN STATIC TESTS

by

Richard N. Tedrick

FOR INTERNAL USE ONLY

NATIONAL AERONAUTICS AND SPACE ADMINISTRATION

GEORGE C. MARSHALL SPACE FLIGHT CENTER

MTP-TEST-MC-61-21

ACOUSTIC FOCAL ZONES AROUND SATURN STATIC TESTS

by

Richard N. Tedrick

GEORGE C. MARHSALL SPACE FLIGHT CENTER

MTP-TEST-MC-61-21

ACOUSTIC FOCAL ZONES AROUND SATURN STATIC TESTS

by

Richard N. Tedrick

ABSTRACT

Meteorologically-caused acoustic focal zones surrounding static test firings of the Saturn vehicle are investigated both theoretically and empirically.

General equations are developed for ray-tracing acoustic signals from their source to points on the earth's surface. Definition is made of boundary conditions which result in the equations' application to the location of the boundaries of the affected areas. The calculated focal zone boundaries are shown for periods covering 16 static test firings of the Saturn at Marshall Space Flight Center and are compared to over-all sound pressure level data taken during the firings at ranges up to 9 miles.

Empirical data are presented showing the rise in over-all sound pressure level resulting from meteorological focusing and showing the effect of both inverse square law and excess attenuation.

TABLE OF CONTENTS

LIST OF ILLUSTRATIONS

LIST OF ILLUSTRATIONS (Cont'd)

GEORGE C. MARSHALL SPACE FLIGHT CENTER

MTP-TEST-MC-61-21

ACOUSTIC FOCAL ZONES AROUND SATURN STATIC TESTS

by

Richard N. Tedrick

SUMMARY

Meteorologically-caused acoustic focal zones surrounding static test firings of the Saturn vehicle are investigated both theoretically and empirically.

General equations are developed for ray-tracing acoustic signals from their source to points on the earth's surface. Definition is made of boundary conditions which result in the equations' application to the location of the boundaries of the affected areas. The calculated focal zone boundaries are shown for periods covering 16 static test firings of the Saturn at Marshall Space Flight Center and are compared to over-all sound pressure level data taken during the firings at ranges up to 9 miles.

Empirical data are presented showing the rise in over-all sound pressure level resulting from meteorological focusing and showing the effect of both inverse square law and excess attenuation.

SECTION I. INTRODUCTION

Several authors (1, 2, 7, and 8) have shown that acoustic energy propagating away from the earth's surface through the atmosphere can, under specified circumstances, be refracted (bent) back toward the ground. In the past, this effect has rarely been of interest because of the limited signal strengths which it was possible to sustain over appreciable periods. However, since the development of the large rocket engine, this refractive effect has assumed greater importance, especially in the civilian areas surrounding the test sites for such large rocket engines.

The acoustical focusing problem posed by the static test firing of the Saturn booster at Marshall Space Flight Center is greater because of the proximity of the city of Huntsville, Alabama. The city is on the north and east boundaries of Redstone Arsenal about 5 to 12 miles from the Saturn Test Tower.

Meteorologically, the MSFC-Huntsville area is dominated by a general westerly-southwesterly prevailing wind pattern. During the winter months, this pattern intensifies and is quite often accompanied by a strong surface temperature inversion. This causes the acoustic velocity profile along the azimuth toward the city to assume proportions similar to FIGURE 1. Naturally, such profiles do not occur every day, nor do they often last more than a few hours. Nevertheless, examination of past meteorological data shows that such focusing conditions may exist for varying lengths of time during any season or month.

There are two methods of reducing such a noise problem. One is to reduce the amount of acoustic energy which is radiated into the atmosphere. The second is to test under meteorological conditions which would not return energy to sensitive areas. Undoubtedly the first approach would allow the various rocket projects more discretion in test scheduling, but since progress in booster construction has exceeded muffler design, there is a need for determining, on a routine day-to-day basis, those areas which may be acoustically affected by large-scale rocket tests.

Toward this end, an analytical method has been developed for the computation of the boundaries of the acoustic focal zones.

SECTION II. THEORY

In order to consider the path of propagation of acoustic energy, it is convenient to utilize the concept of the "ray", i.e., an infinitely small segment of the acoustical wave front. This ray traces a pattern which may be called the ray path as it moves through the medium along with the rest of the wave. At each point the wave is normal to the ray path through that point.

The ray, because of its incremental dimensions, can be mathematically treated in the same way as the light ray in optics. Not only does this device enable the acoustician to simplify his computational procedures, but by relating the convergence or divergence of the rays to the normally-assumed spherical radiation, he can approximate the gain or loss in signal strength due to such refraction.

Snell's Law, when applied to acoustical energy travelling through a horizontally-stratified atmosphere where each layer of such an atmosphere contains a constant velocity gradient, takes the form:

$$\cos \theta = \frac{C}{C_{max}} ; \; C_{max} = \frac{C}{\cos \theta} . \qquad (1)$$

θ is the angle which the ray makes with the horizontal at the altitude where the velocity of sound along the path of propagation is C. C_{max} is the acoustic velocity at the altitude where the ray path is horizontal. (3)

Equation 1 states that if the attitude (angle from the horizontal) and the velocity of sound at some given altitude is known, the attitude of the ray may be calculated for every height where the velocity of sound is known. Thus, all that is needed to trace the path of a sound ray as it moves through the atmosphere is the acoustic velocity profile and one measured or defined angle.

If one is interested in certain well-defined boundary conditions where (by definition) the attitude is known, then it is possible to determine the ray paths defined by those conditions. The intersection of these ray paths with the earth's surface will define the boundaries of the intersection of the entire acoustic wave front with the ground.

The aforementioned problem here is one of locating the boundaries of one or more zones which may be subjected to focusing of acoustic energy. These boundary conditions may be defined within the accuracy limits placed upon the problem by the meteorological data acquisition techniques. The boundaries may be considered to be determined by two angles; the minimum and the maximum angles with which energy can originate at the source and be refracted back to earth in a single continuous wave. If there are several waves (or more precisely, several portions of the same acoustic front) which return to earth, a corresponding rise occurs in the number of boundaries to be calculated.

The velocity profile may be assumed to follow the general pattern shown in FIGURE 2 in those cases in which focusing is important. Of course, this pattern may vary or may be composed of a number of smaller layers which follow the general trend of FIGURES 2 and 3. In some cases the altitude, h_1, may be zero.

Assuming an acoustic source at the surface, the lowest possible angle of transmission is zero degrees. Because an acoustic front bends toward the lower velocity end of any gradient when C_1 is less than C_o, this grazing ray will curve upward. At height h_1, the velocity of sound is C_1 and the attitude of the ray may be expressed:

$$\cos \theta = C_1/C_{max} \tag{2}$$

However, for this ray, C_{max} is equal to C_o since the sound travels horizontally at the surface. Equation 2 then becomes:

$$\cos \theta = C_1/C_o \tag{3}$$

It may be seen that at height, h_b, where C is equal to C_o, cos θ equals unity and, therefore, the boundary ray has been bent to the horizontal. Since any increment of positive gradient above the level, h_b, would cause the cosine to be greater than one, h_{b1} may be considered as the zenith altitude of one of the boundary rays.

In a layer of thickness, h, bounded by velocities C_n and C_n+1 and containing a constant velocity gradient, the ray path follows an arc of a circle which is subtended by the angles θ_n and θ_{n+1} as shown in FIGURE 4 The horizontal distance traversed by the sound in the layer is given by the equation:

$$X = \frac{h}{\tan \frac{(\theta_n + \theta_{n+1})}{2}} \tag{4}$$

Since, assuming a horizontally-stratified atmosphere, the acoustic ray passes twice through each layer, the horizontal distance, R, from the source to the reincident point is equal to twice the summation of X.

$$R = 2 \sum_{c = 0}^{C = C_{max}} X \tag{5}$$

Another boundary of the reincident energy zone may be found by considering the maximum angle of transmission which can result in energy being refracted back to earth. This will occur to the ray which is horizontal at the maximum velocity. Equation 1, for the condition in FIGURE 1, then becomes:

$$\cos \theta_o = \frac{C_o}{C_2} \tag{6}$$

Using this new value of θ_o in Equations 4 and 5, R is calculated in the same way as above.

The atmosphere sometimes becomes fairly complex and the resulting acoustic velocity profiles then may contain several local maxima and minima below the over-all maximum. By definition, a maximum point on the sound velocity profile is one where, above and below it in altitude, the velocity is less than at that point, or put another way, any level which has a positive gradient beneath and a negative gradient above. Since the negative gradient will bend the sound upward while the positive gradient bends it down, there will result a dead zone from that altitude to some point on the ground.

Significant levels are those altitudes at which occur the above-mentioned maxima and minima. With the exception of the over-all maximum, for each local maximum there is some altitude above it at which the velocity equals that local maximum. This is a boundary level. There is a radius, R, to be calculated for each maximum and each boundary level. Thus, in FIGURE 2, there would be two reincident focal zones; one bounded by the values of R calculated for heights H_{b1} and h_a, the other by values of R for heights h_{b2} and h_2.

In FIGURE 3, the meteorological conditions for the MSFC-Huntsville area at 1640 CST on December 20, 1960 are shown. Along an azimuth of 35 degrees from the source, local maxima occur at 500 and 1,500 feet above the surface and result in dead zones in the surface from 10 to 20 thousand feet and 27 to 49 thousand feet range, respectively. The over-all maximum occurs at a 5,000-foot altitude. Assuming an idealized hemispherical sound source at the surface, any sound generated on the initial hemisphere with an angle greater than 18 degrees 48 minutes would not have returned to the ground within the first 80,000 feet (approximately 15 miles). It is possible that positive gradients above the arbitrarily-chosen 10,000-foot ceiling on meteorological observations may have caused acoustic focusing beyond this range. However, the path length to such focal regions would have been sufficiently long to attenuate the acoustic signal below the damage and personnel irritation levels.

Up to this point, it has been assumed that the velocity profile is known. Usually the only informational input is from radiosonde data. This gives, in tabular form, the temperature, T, and the wind speed, V, and direction, oc, as functions of altitude, H, above mean sea level.

Since the wind is a vectorial quantity, the effect of the wind upon the velocity of sound propagation is affected by the wind direction, α, and the azimuth, β, along which the various R's will be calculated. If γ is defined as the angle between α and β then:

$$C = 1052 + 1.106T + 1.467V \cos\gamma,$$

where V is in miles per hour, T in degrees Fahrenheit, and C in feet per second.

If γ is less than 90 degrees, then the sign of V cos γ is negative.

Thus, because of the effect of the wind directions in the various layers, the acoustic velocity profiles will vary with azimuth and the values of R will need to be recalculated for each applicable azimuth.

SECTION III. DISCUSSION

In order to have useful and effective plots of the focal zones, it was decided that acoustic velocity profiles needed to be calculated for each 5 degrees of azimuth. Since there are 21 meteorological data levels, this results in the value of C being calculated 1,512 times from Equation 7. Actually, over 50,000 separate calculations have to be made for each run in order to compute every value of the radius, R, resulting from just the first 10,000 feet of meteorological data. For obvious reasons, the boundary zone problem was programmed for a digital computer.

The acoustic focal zone boundaries for Saturn tests SAT-01 through SAT-13 and SA-01 through SA-03 are shown in FIGURES 5 through 20. The meteorological data from which these boundaries were calculated are shown in TABLE I. These data were taken from radiosonde balloon flights. They are presented in TABLE I.

Because of the wide range of azimuths from the Saturn test tower to the Huntsville city limits, only about 31 percent of the tests were performed at times where no focusing at all occurred within the city limits. However, no evidence of refracted sound in the main downtown area was found in approximately 80 percent of the firings.

In order to better judge the effects of meteorological focusing, MSFC personnel were assigned to monitor various locations with sound-level measuring equipment during later test periods. The results of these measurements are shown along with the focal areas in FIGURES 14 through 20. As can be seen, the measurements generally agree with the predicted focal areas. The boundaries appear to be fairly well-defined but are subject to some shadow zone diffusion. This diffusion may be explained by Huygen's principle which states that no finite energy wave travelling in an infinite homogeneous medium may travel in only one direction since each point on the wave front acts as a new point source. There would be, consequently, some energy spill-out into any shadow zone.

The far-field measurements are shown in FIGURES 21 through 28. The eight-engine Saturn C-1 configurations which were tested had a nominal thrust of 1.3 million pounds and an acoustic efficiency of approximately 0.7 percent. SAT-10 was only a two-engine test. Included for reference in these figures are the curves for inverse square law attenuation and attenuation due to humidity and molecular absorption.(4) The latter attentuation curve was based rather arbitrarily upon a loss of 4db sound pressure (SPL) per mile. This figure appears to fit the empirical data reasonably well.

However, it can be seen that this particular loss figure is quite weather-dependant and is subject to some rather rapid changes upon entering focal zones. It would appear from consideration of the empirical SPL data that the result of one or more focal areas is the upward shift of the whole SPL curve a certain number of decibels. It appears also that these shifts are additive, resulting in an apparent rise in the sound pressure level of the source.

The focal conditions noted resulted in appropriate rises in measured sound pressure levels. However, during SAT-12, an abrupt rise was noted at approximately two miles from the source along an azimuth where no focus was anticipated. One possible explanation of such an occurrence lies in the manner in which the meteorological data are reduced. The data are presently provided at fixed 500-foot altitude increments because of the requirements of other projects utilizing the data. If the maxima and minima which are of interest do not appear at those precise levels, then they are, to all extents, lost and only the larger trends become discernible. Since normally the most violent of these local inhomogenities occur near the surface, their results could be expected to become evident within the first few miles.

Thus, if somewhere between the 1,000- and 1,500-foot boundaries, there existed a layer which contained a wind only 5 to 7 miles per hour higher than that measured at the 1,500-foot boundary, the calculated focal area boundary would have been several miles nearer than that shown in FIGURE 16. Such an occurrence may be strongly suspected from the levels measured. The above gap in the data might thus be resolved if the meteorological parameters were reported in what the U. S. Weather Bureau calls "significant levels", i.e., important local maxima and minima. Such a presentation would probably also increase the accuracy with which the known layer boundaries are calculated, since they also are calculated from the acoustic velocity at the nearest 500-foot level.

SECTION IV. SUMMARY, CONCLUSIONS, AND RECOMMENDATIONS

Analytically, it is possible to calculate, within the limitations of the available meteorological data, the boundaries of areas in which acoustical focusing is likely to occur. Such focusing, in the case of boosters of the Saturn class, may result in increases in sound pressure level of up to 30 decibels. By judicious monitoring of the meteorological parameters, it should be possible to conduct large-scale booster tests with no adverse community reaction.

It appears, on the basis of presently available data, that the noise from Saturn static test firings is attenuated at a rate approximately equal to that of the inverse square law plus an excess attenuation of 4 decibels per mile for at least the first 9 miles.

Work should proceed toward the development of an accurate means of predetermining the sound pressure level distribution within focal areas which are located by this method.

TABLE I

	ALTITUDE (FT)	TEMP (°F)	WIND DIR.	WIND MPH
TEST: SAT-1	Surface	68.2	315	12
DATE: 3-28-60	500	66.0	300	13
TIME: 0900	1000	64.0	260	15
	1500	61.9	280	16
	2000	60.4	290	15
	2500	57.7	240	16
	3000	56.3	240	17
	3500	53.8	240	17
	4000	53.3	240	16
	4500	50.0	230	14
	5000	48.7	230	14
	5500	46.6	230	12
	6000	45.0	230	12
	6500	42.8	230	12
	7000	41.0	230	12
	7500	39.5	230	12
	8000	38.1	230	12
	8500	36.7	230	13
	9000	35.4	230	15
	9500	33.7	230	14
TEST: SAT-2	Surface	77.5	205	18
DATE: 4-6-60	500	74.3	215	20
TIME: 1605	1000	71.6	225	23
	1500	68.0	240	26
	2000	64.7	240	30
	2500	63.7	245	33
	3000	60.1	250	35
	3500	57.6	255	40
	4000	56.3	260	42
	4500	53.9	260	46
	5000	52.0	265	49
	5500	50.2	265	58
	6000	48.2	270	57
	6500	46.4	270	56
	7000	44.0	280	53
	7500	42.8	285	50
	8000	40.6	290	49
	8500	38.7	295	49
	9000	36.5	300	49
	9500	34.1	300	49

TABLE I. (Cont'd)

	ALTITUDE (FT)	TEMP (°F)	WIND DIR.	WIND MPH
TEST: SAT-3	Surface	79.2	290	10
DATE: 4-29-60	500	77.0	285	13
TIME: 1745	1000	75.2	285	15
	1500	73.0	290	16
	2000	69.1	280	16
	2500	68.0	280	16
	3000	66.2	280	17
	3500	65.3	275	17
	4000	60.8	270	19
	4500	56.3	250	16
	5000	53.6	235	19
	5500	51.8	225	21
	6000	50.0	220	23
	6500	48.2	220	24
	7000	47.3	220	24
	7500	46.4	220	25
	8000	45.5	220	25
	8500	45.0	220	26
	9000	44.2	220	28
	9500	43.7	220	29
TEST: SAT-4	Surface	86.3	200	6
DATE: 5-17-60	500	83.5	220	9
TIME: 1700	1000	80.1	245	10
	1500	76.8	275	12
	2000	73.4	275	13
	2500	70.0	270	13
	3000	67.6	270	13
	3500	65.3	275	14
	4000	62.6	275	16
	4500	60.2	280	17
	5000	58.1	280	19
	5500	57.0	285	21
	6000	57.0	285	21
	6500	60.9	290	21
	7000	59.3	290	21
	7500	57.9	290	21
	8000	56.0	290	22
	8500	54.6	290	21
	9000	52.0	290	22
	9500	49.8	285	23

TABLE I. (Cont'd)

	ALTITUDE (FT)	TEMP (°F)	WIND DIR.	WIND MPH
TEST: SAT-5	Surface	75.2	120	4
DATE: 5-26-60	500	73.4	140	12
TIME: 1700	1000	71.6	160	20
	1500	69.4	170	25
	2000	67.6	180	26
	2500	65.7	190	27
	3000	63.7	195	28
	3500	61.5	205	27
	4000	57.7	210	27
	4500	57.5	220	27
	5000	55.6	225	26
	5500	53.6	225	25
	6000	51.8	230	23
	6500	49.8	235	23
	7000	47.5	225	24
	7500	45.5	220	25
	8000	43.5	220	26
	8500	41.6	220	27
	9000	40.1	220	27
	9500	37.4	220	23
TEST: SAT-6	Surface	75.4	xxx	calm
DATE: 6-3-60	500	74.1	xxx	calm
TIME: 1700	1000	72.1	xxx	calm
	1500	70.7	45	5
	2000	68.7	30	7
	2500	66.6	20	10
	3000	64.6	15	13
	3500	63.0	10	16
	4000	61.1	10	16
	4500	59.3	5	16
	5000	57.4	360	15
	5500	55.4	350	14
	6000	53.6	350	12
	6500	51.8	350	9
	7000	49.8	360	6
	7500	48.0	10	4
	8000	45.5	10	5
	8500	44.2	10	8
	9000	42.8	10	10
	9500	41.3	10	13

TABLE I. (Cont'd)

	ALTITUDE (FT)	TEMP (°F)	WIND DIR.	WIND MPH
TEST: SAT-7	Surface	86.0	xxx	calm
DATE: 6-8-60	500	82.4	xxx	calm
TIME: 1700	1000	79.2	xxx	calm
	1500	76.6	20	8
	2000	73.6	20	8
	2500	71.6	25	7
	3000	69.4	30	6
	3500	66.3	30	5
	4000	64.5	30	5
	4500	62.4	20	4
	5000	60.2	25	4
	5500	57.6	30	4
	6000	55.4	45	4
	6500	52.7	50	6
	7000	51.6	55	7
	7500	50.0	55	8
	8000	48.4	55	9
	8500	47.7	55	7
	9000	46.2	45	7
	9500	44.6	45	8
TEST: SAT-8	Surface	83.3	350	4
DATE: 6-15-60	500	82.0	350	12
TIME: 1700	1000	80.7	350	11
	1500	79.4	350	10
	2000	78.1	330	10
	2500	76.8	300	11
	3000	75.5	280	15
	3500	74.2	260	22
	4000	72.9	260	30
	4500	71.9	270	40
	5000	70.3	270	40
	5500	69.0	270	38
	6000	67.7	265	35
	6500	66.4	260	32
	7000	66.1	245	30
	7500	65.8	240	29
	8000	64.5	240	30
	8500	63.2	210	33
	9000	61.9	200	36
	9500	60.6	190	40

TABLE I. (Cont'd)

	ALTITUDE (FT)	TEMP (°F)	WIND DIR.	WIND MPH
TEST: SAT-9	Surface	45.5	xxx	calm
DATE: 12-2-60	500	42.9	xxx	calm
TIME: 1650	1000	41.4	xxx	calm
	1500	39.3	210	3
	2000	37.9	180	4
	2500	38.8	155	6
	3000	39.4	130	7
	3500	40.6	130	9
	4000	41.3	135	9
	4500	41.3	150	7
	5000	40.1	160	7
	5500	38.6	190	5
	6000	37.0	210	6
	6500	35.4	230	8
	7000	33.8	245	10
	7500	32.0	240	11
	8000	30.4	235	12
	8500	28.8	240	12
	9000	27.5	250	14
	9500	25.9	260	14
TEST: SAT-10	Surface	51.6	330	6
DATE: 12-10-60	500	50.7	310	8
TIME: 1604	1000	50.7	310	14
	1500	50.9	305	13
	2000	50.0	290	13
	2500	48.4	290	14
	3000	46.9	285	15
	3500	45.3	280	16
	4000	44.1	275	17
	4500	42.3	275	17
	5000	41.6	265	17
	5500	40.8	255	18
	6000	41.0	250	16
	6500	41.7	240	15
	7000	41.9	250	16
	7500	41.2	250	17
	8000	40.6	240	19
	8500	39.4	240	21
	9000	38.1	240	22
	9500	37.6	230	23

TABLE I. (Cont'd)

	ALTITUDE (FT)	TEMP (°F)	WIND DIR.	WIND MPH
TEST: SAT-11	Surface	51.4	210	8
DATE: 12-20-60	500	50.0	190	30
TIME: 1640	1000	49.8	175	37
	1500	48.7	185	48
	2000	47.8	180	49
	2500	46.7	190	50
	3000	45.3	195	52
	3500	44.1	205	54
	4000	42.8	210	57
	4500	41.2	215	58
	5000	40.1	215	60
	5500	38.8	220	60
	6000	37.4	220	60
	6500	35.9	220	61
	7000	34.3	225	58
	7500	33.2	225	50
	8000	30.7	225	55
	8500	29.5	220	57
	9000	27.5	220	62
	9500	26.1	220	66
TEST: SAT-12	Surface	45.5	240	4
DATE: 1-31-61	500	44.1	240	5
TIME: 1700	1000	42.7	230	12
	1500	41.6	235	15
	2000	40.5	240	17
	2500	39.2	250	17
	3000	38.0	260	16
	3500	36.9	270	17
	4000	37.8	275	23
	4500	39.0	280	27
	5000	39.0	280	35
	5500	38.5	280	41
	6000	39.9	285	42
	6500	42.7	290	42
	7000	43.2	295	35
	7500	43.2	300	28
	8000	41.0	305	23
	8500	39.2	305	23
	9000	37.2	295	24
	9500	35.0	295	26

TABLE I. (Cont'd)

	ALTITUDE (FT)	TEMP (°F)	WIND DIR.	WIND MPH
TEST: SAT-13	Surface	65.7	xxx	calm
DATE: 2-14-61	500	63.3	xxx	calm
TIME: 1645	1000	61.3	xxx	calm
	1500	59.4	270	22
	2000	57.4	230	29
	2500	55.6	230	29
	3000	53.6	235	36
	3500	51.6	250	36
	4000	49.6	260	36
	4500	47.8	270	45
	5000	45.9	270	51
	5500	43.5	270	67
	6000	41.7	270	67
	6500	39.7	270	74
	7000	37.7	270	74
	7500	40.8	270	81
	8000	41.0	270	81
	8500	39.0	270	81
	9000	37.2	270	87
	9500	35.1	270	87
TEST: SA-01	Surface	66.9	xxx	calm
DATE: 4-29-61	500	64.2	xxx	calm
TIME: 1638	1000	61.3	260	2
	1500	58.8	270	2
	2000	55.9	280	4
	2500	53.4	290	4
	3000	50.4	300	4
	3500	47.7	310	7
	4000	45.1	315	11
	4500	42.4	315	15
	5000	41.7	310	25
	5500	41.7	305	31
	6000	39.2	300	38
	6500	39.2	300	40
	7000	37.6	295	40
	7500	36.1	295	40
	8000	34.9	295	40
	8500	33.4	295	43
	9000	32.2	295	43
	9500	35.1	295	45

TABLE I. (Cont'd)

	ALTITUDE (FT)	TEMP (°F)	WIND DIR.	WIND MPH
TEST: SA-02	Surface	84.7	200	11
DATE: 5-5-61	500	81.9	195	16
TIME: 1610	1000	79.2	190	20
	1500	76.6	190	18
	2000	73.6	190	16
	2500	70.9	190	16
	3000	68.2	190	16
	3500	66.7	195	18
	4000	63.7	185	20
	4500	61.0	185	22
	5000	58.8	185	27
	5500	57.0	190	31
	6000	55.6	200	34
	6500	53.4	205	36
	7000	52.7	215	36
	7500	51.4	225	34
	8000	48.9	230	34
	8500	46.9	235	36
	9000	45.1	235	36
	9500	43.5	235	40
TEST: SA-03	Surface	76.1	120	5
DATE: 5-11-61	500	72.7	110	9
TIME: 1550	1000	69.8	100	16
	1500	66.2	100	18
	2000	63.3	105	20
	2500	60.4	100	20
	3000	57.4	100	22
	3500	55.0	95	22
	4000	52.5	95	20
	4500	50.0	95	20
	5000	48.4	90	18
	5500	46.6	80	18
	6000	44.8	75	18
	6500	43.0	70	20
	7000	40.8	60	22
	7500	39.0	50	18
	8000	36.3	50	20
	8500	34.5	50	20
	9000	32.2	50	25
	9500	30.4	50	27

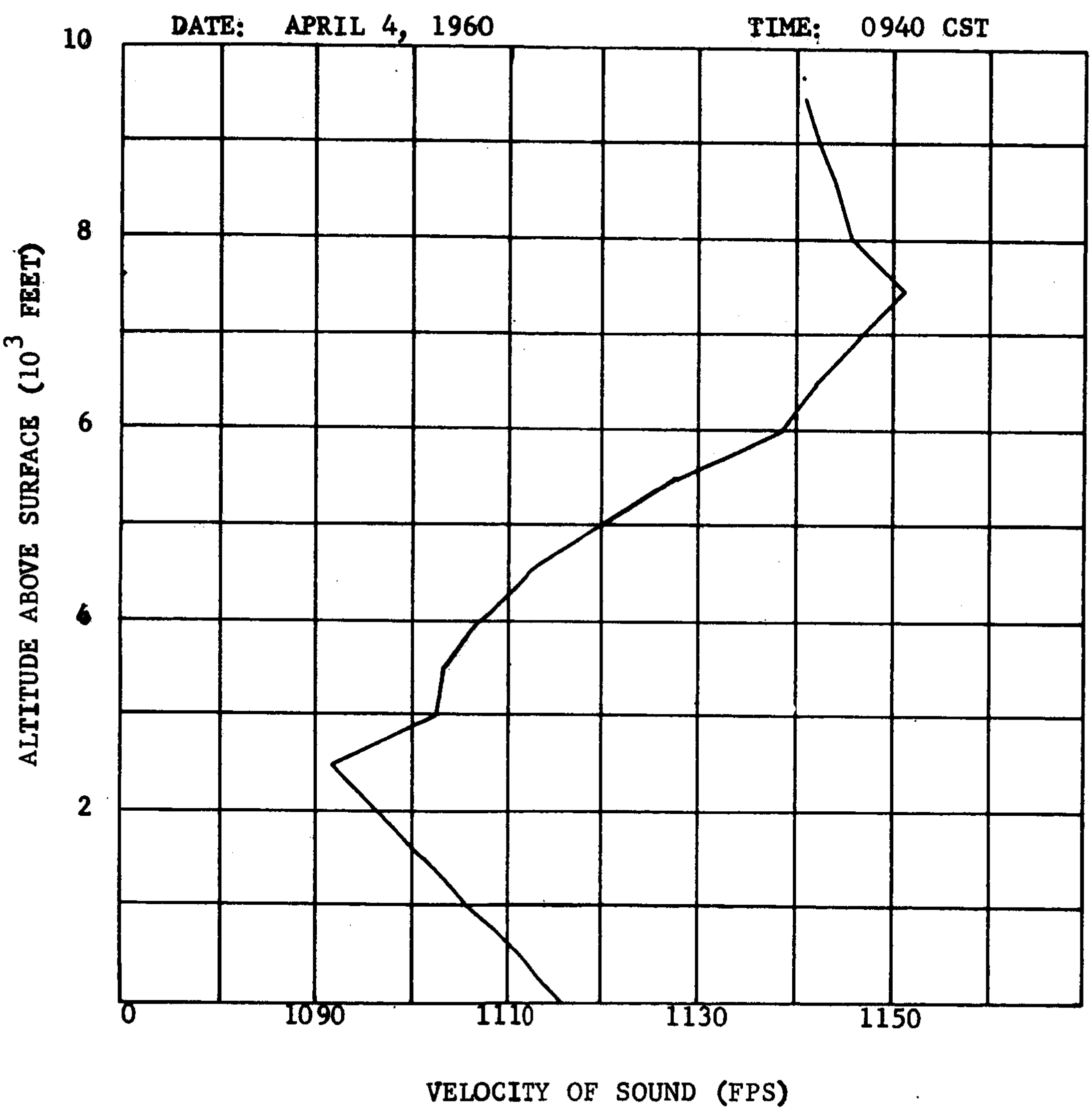

FIGURE 1. VELOCITY OF SOUND PROFILE TOWARD HUNTSVILLE

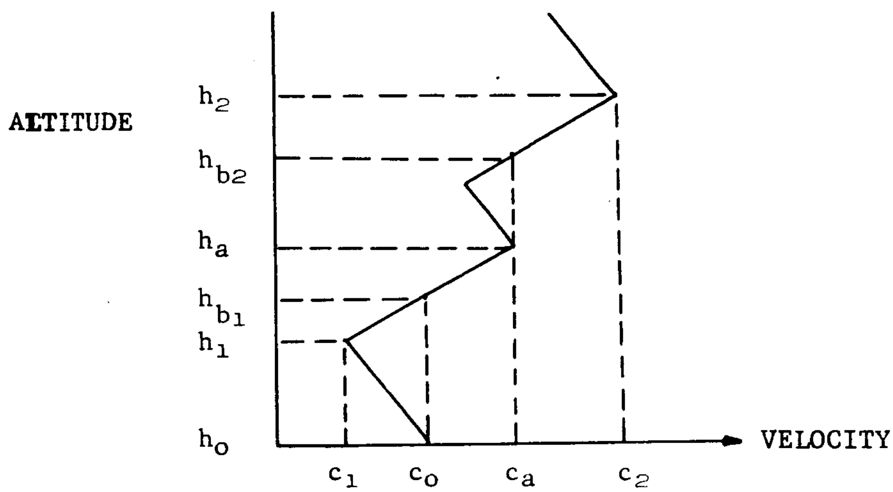

FIGURE 2. CALCULATED SOUND RAYS FOR SATURN TEST - DECEMBER 20, (ALTITUDE VERSUS VELOCITY)

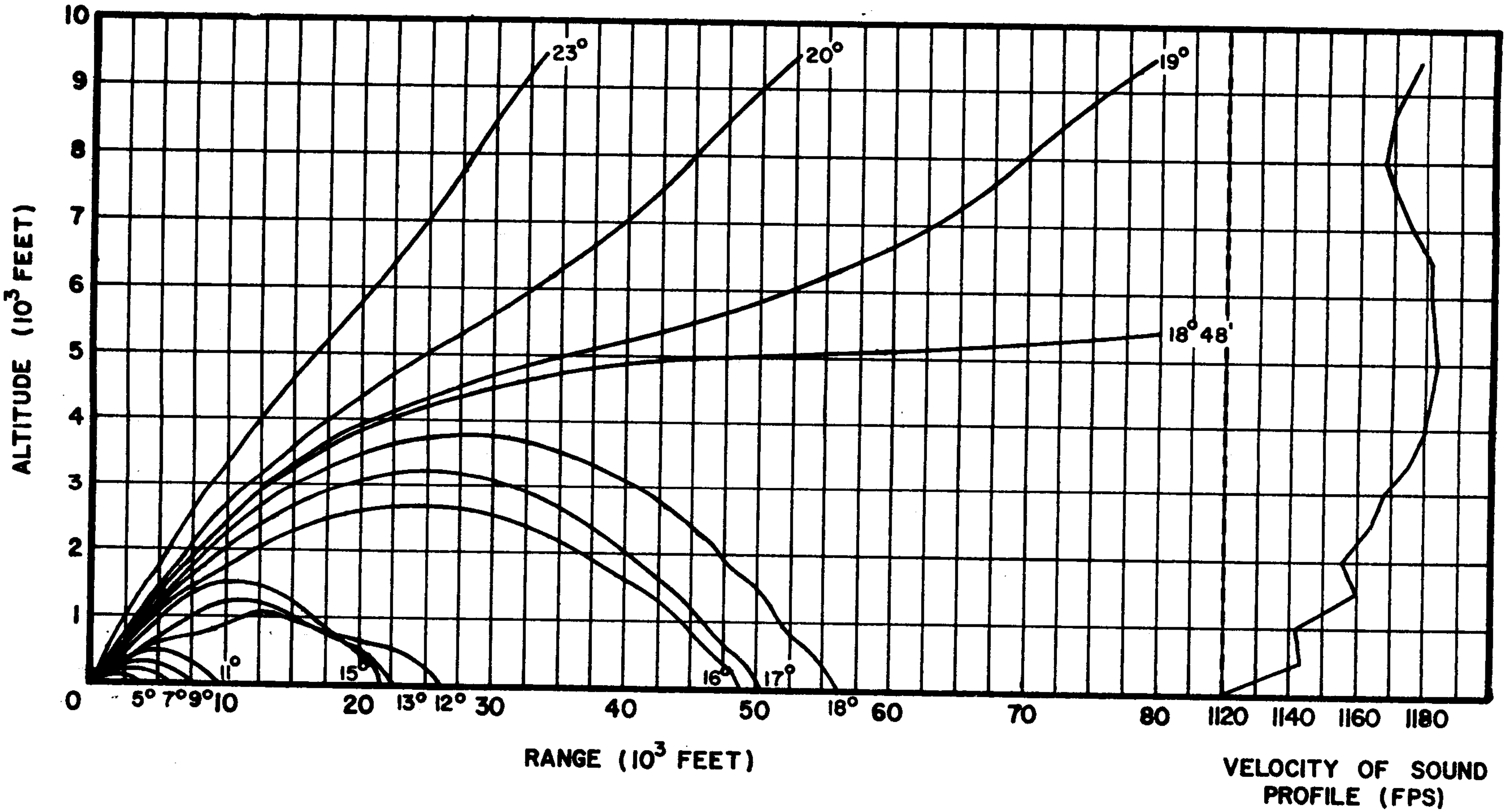

FIGURE 3. CALCULATED SOUND RAYS FOR SATURN TEST - DECEMBER 20, 1960 (ALTITUDE VERSUS RANGE)

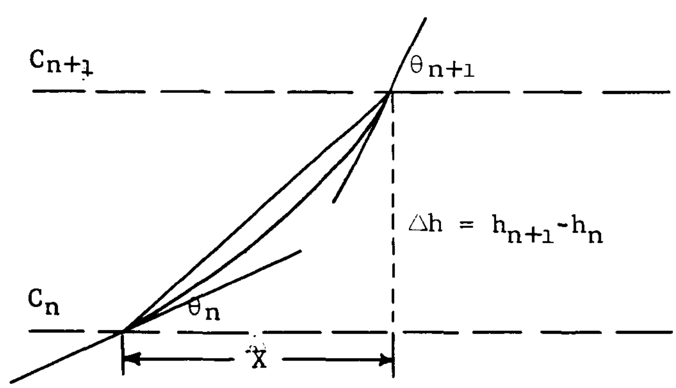

FIGURE 4. RAY PATH

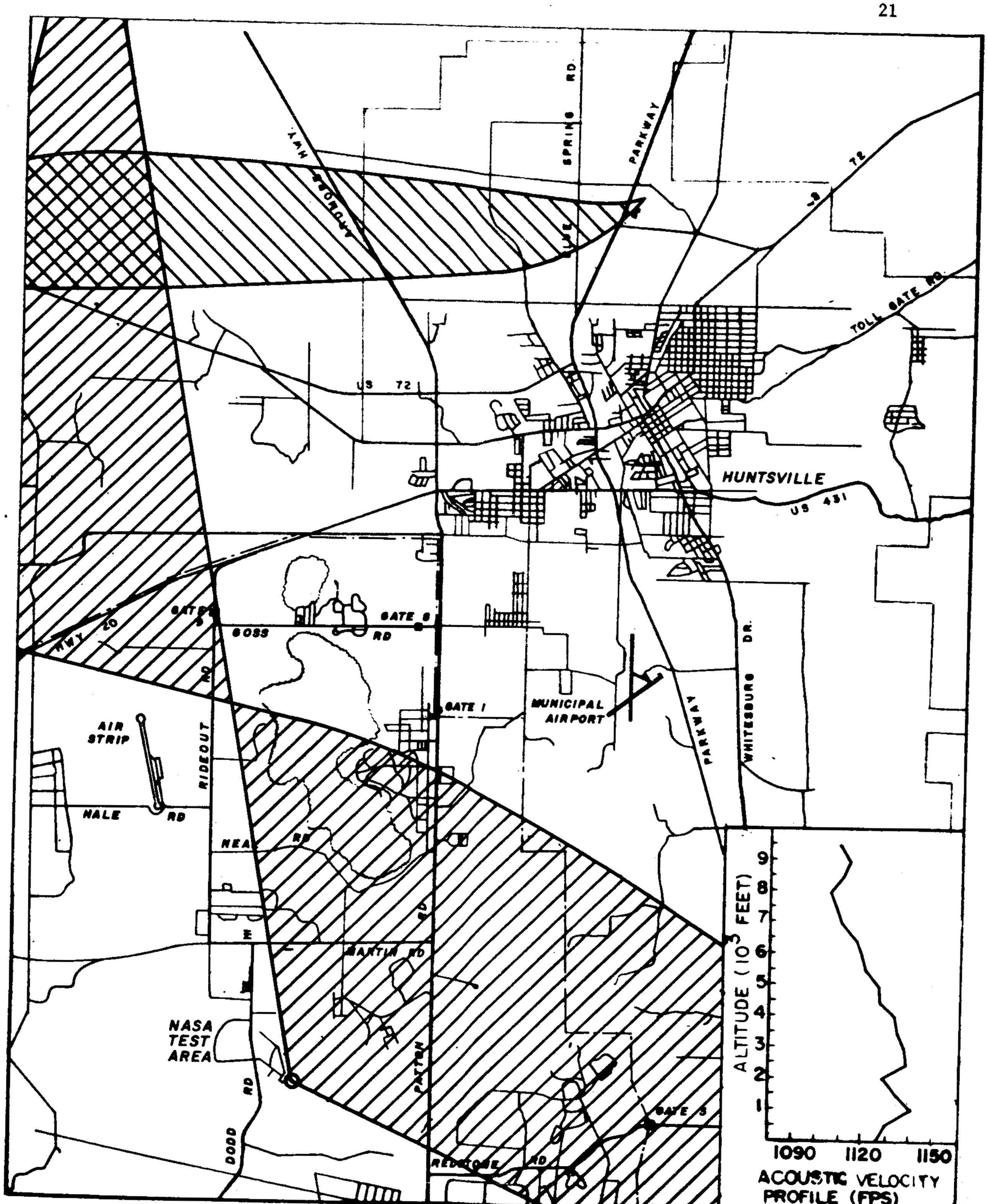

FIGURE 5. TEST SAT-01, MARCH 3, 1960

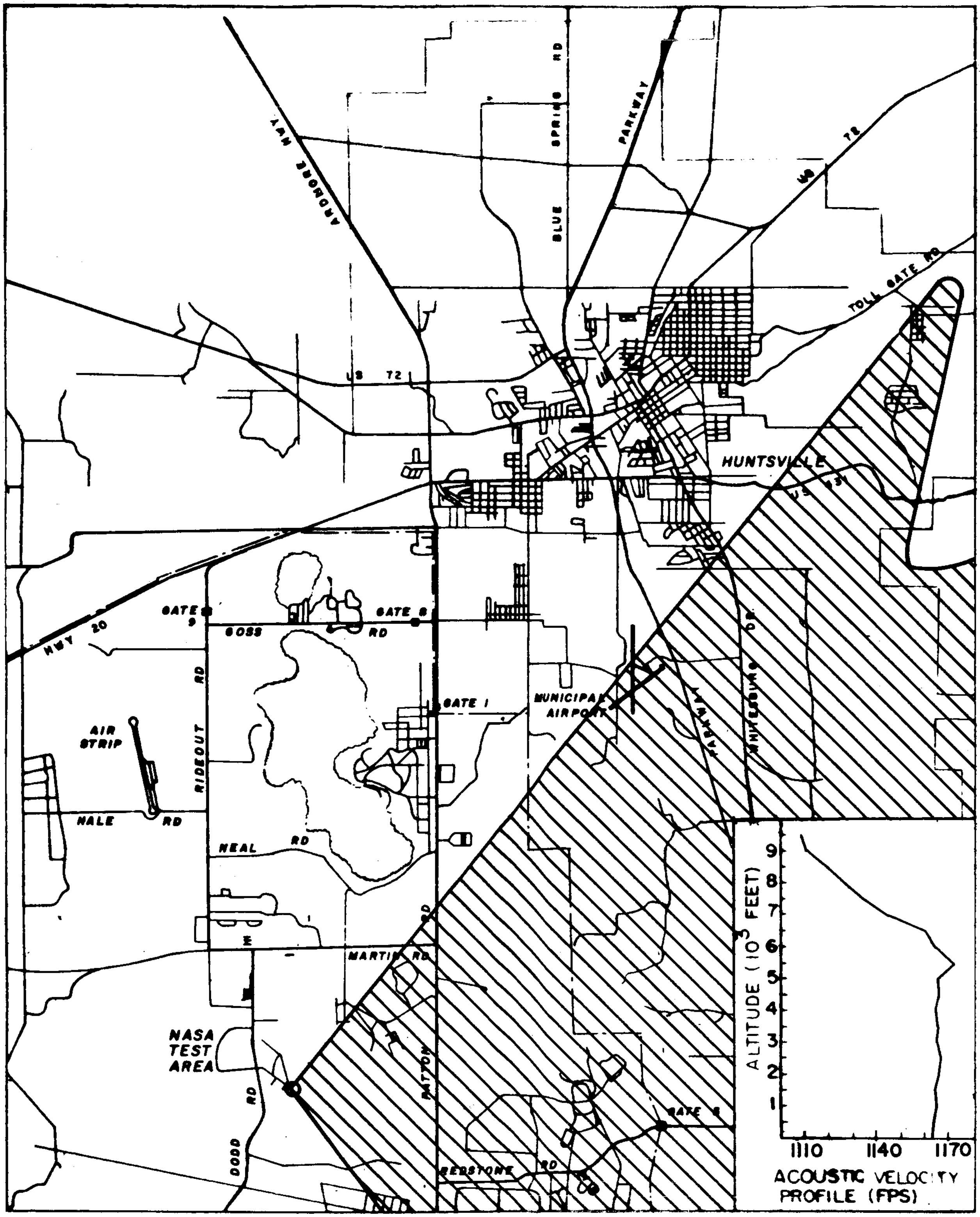

FIGURE 6. TEST SAT-02, APRIL 6, 1960

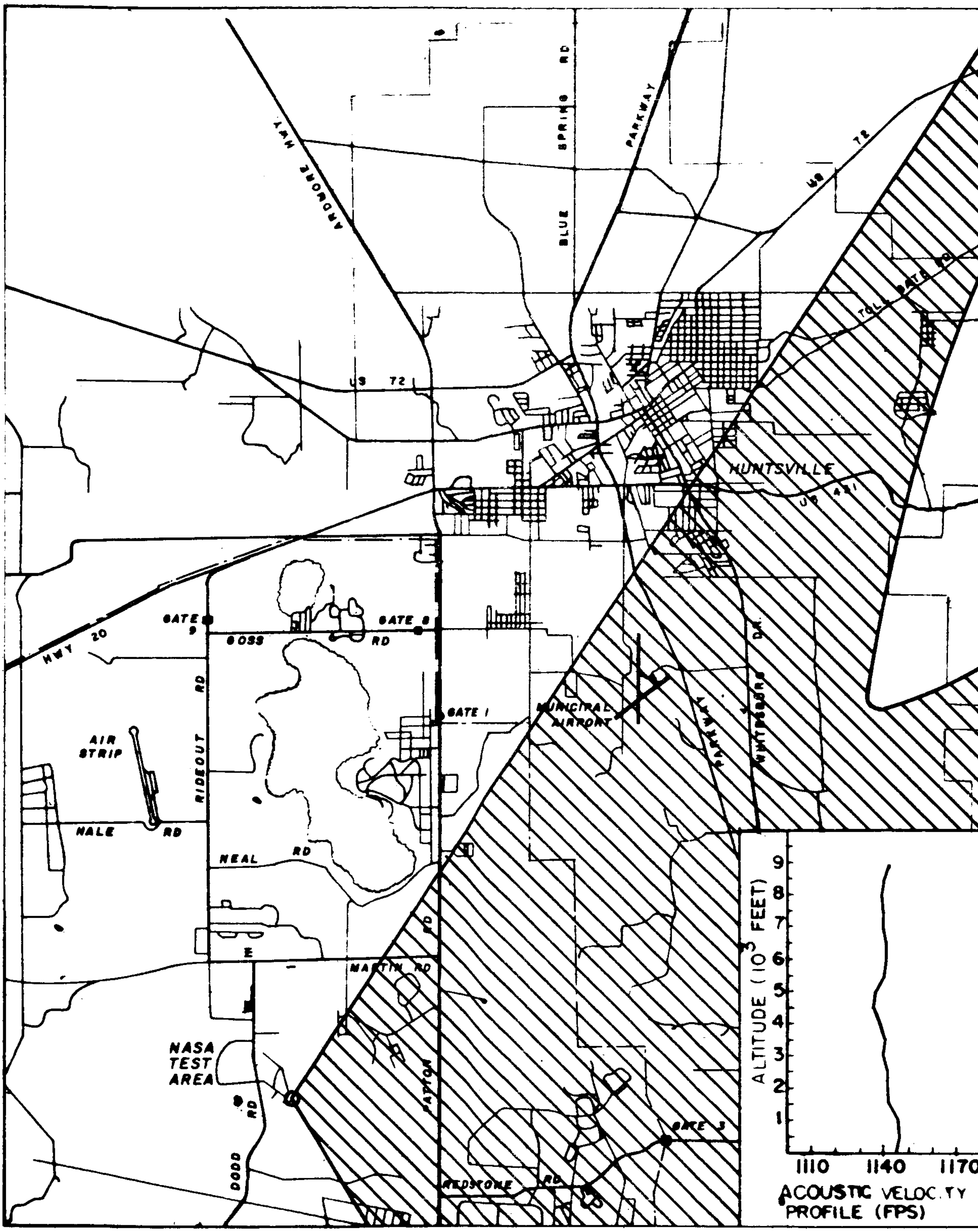

FIGURE 7. TEST SAT-03, APRIL 29, 1961

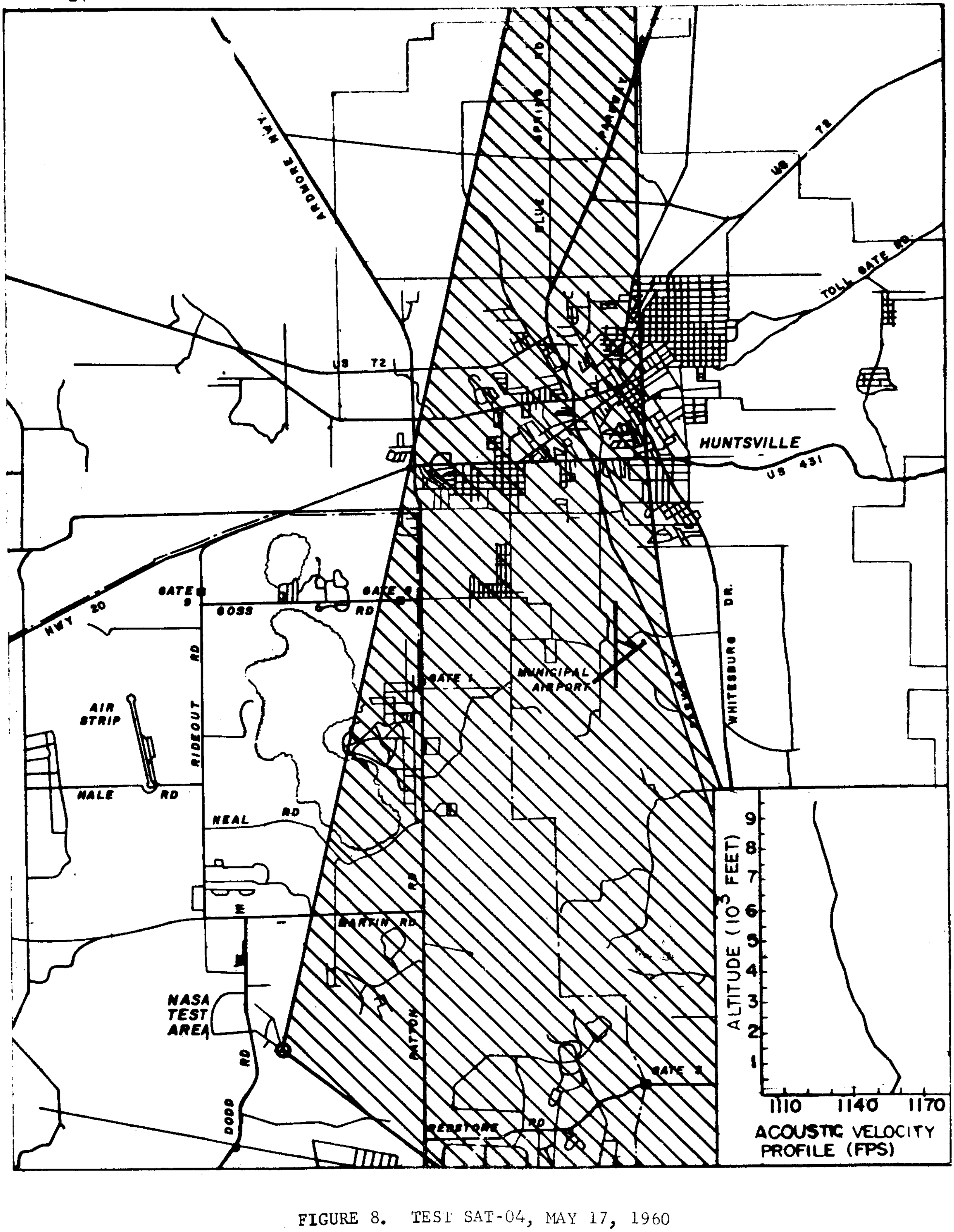

FIGURE 8. TEST SAT-04, MAY 17, 1960

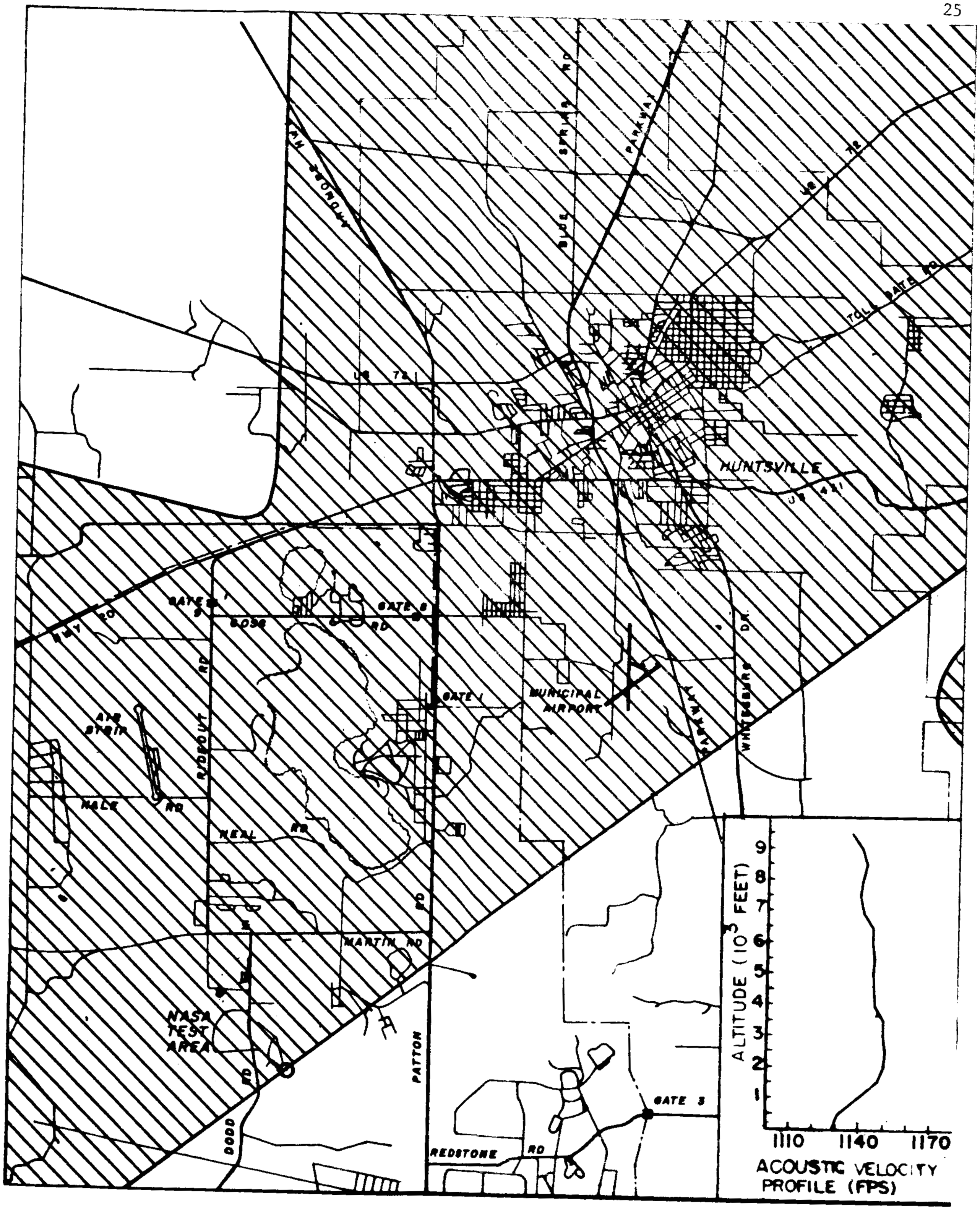

FIGURE 9. TEST SAT-05, MAY 26, 1960

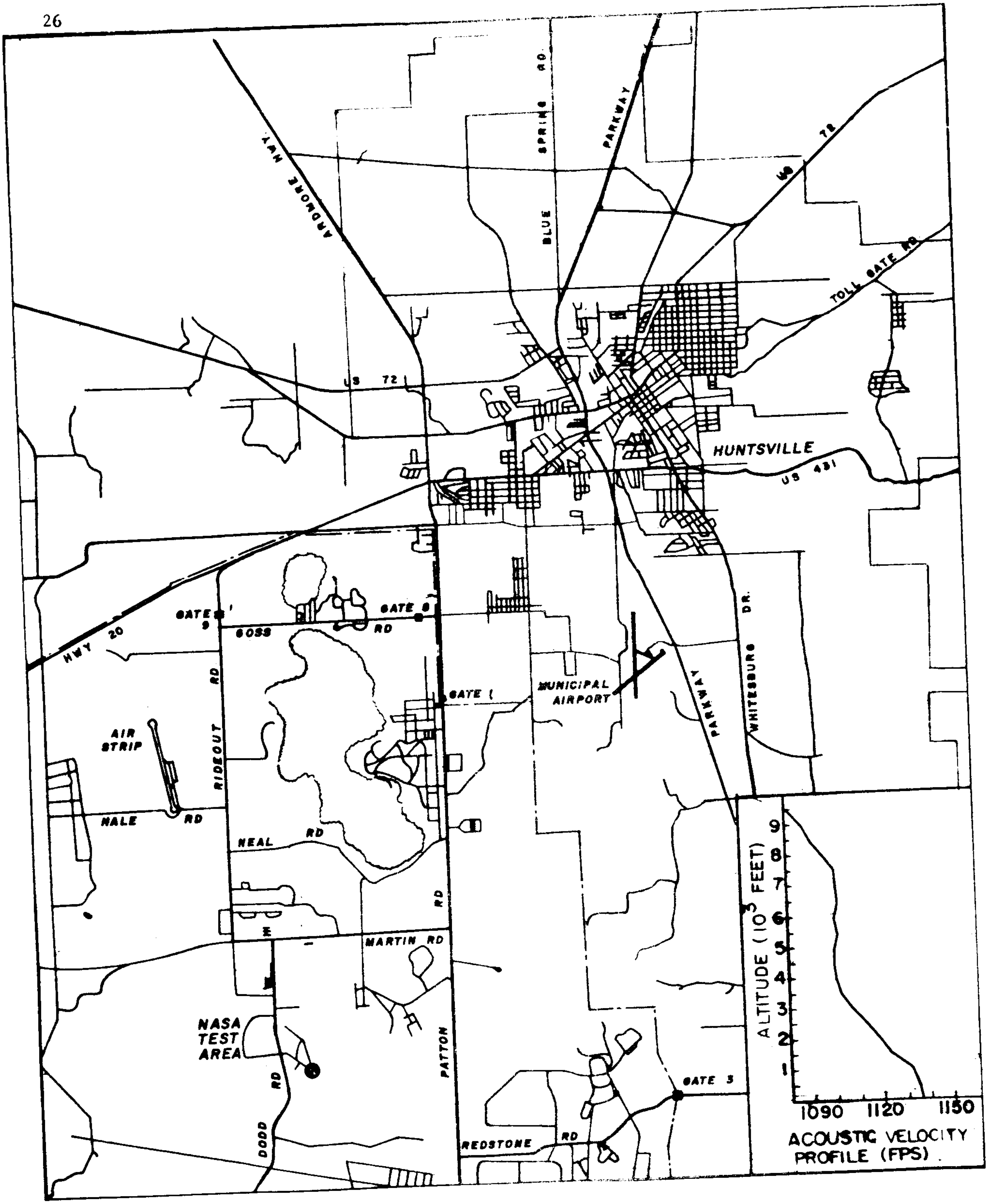

FIGURE 10. TEST SAT-06, JUNE 3, 1960

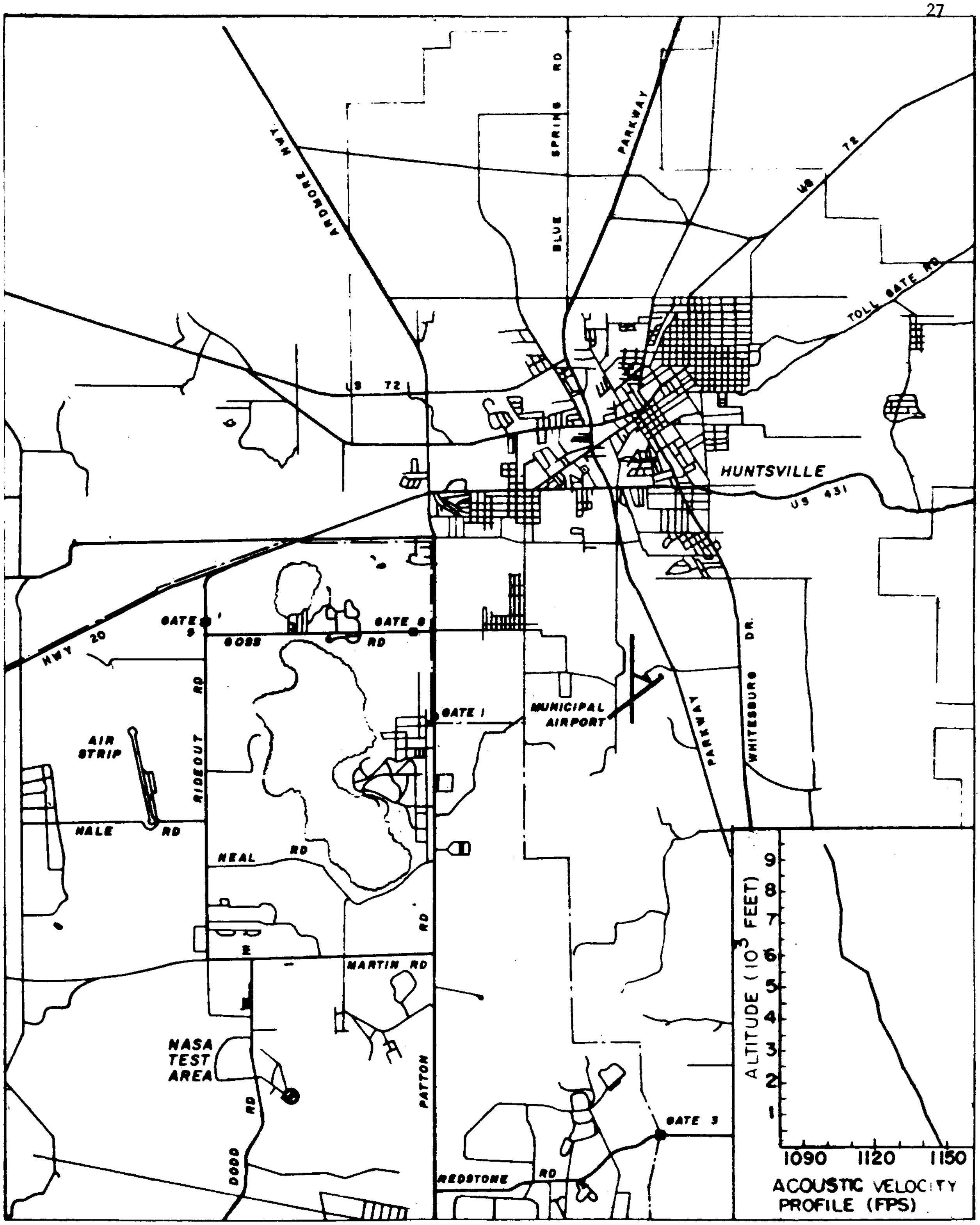

FIGURE 11. TEST SAT-07, JUNE 8, 1960

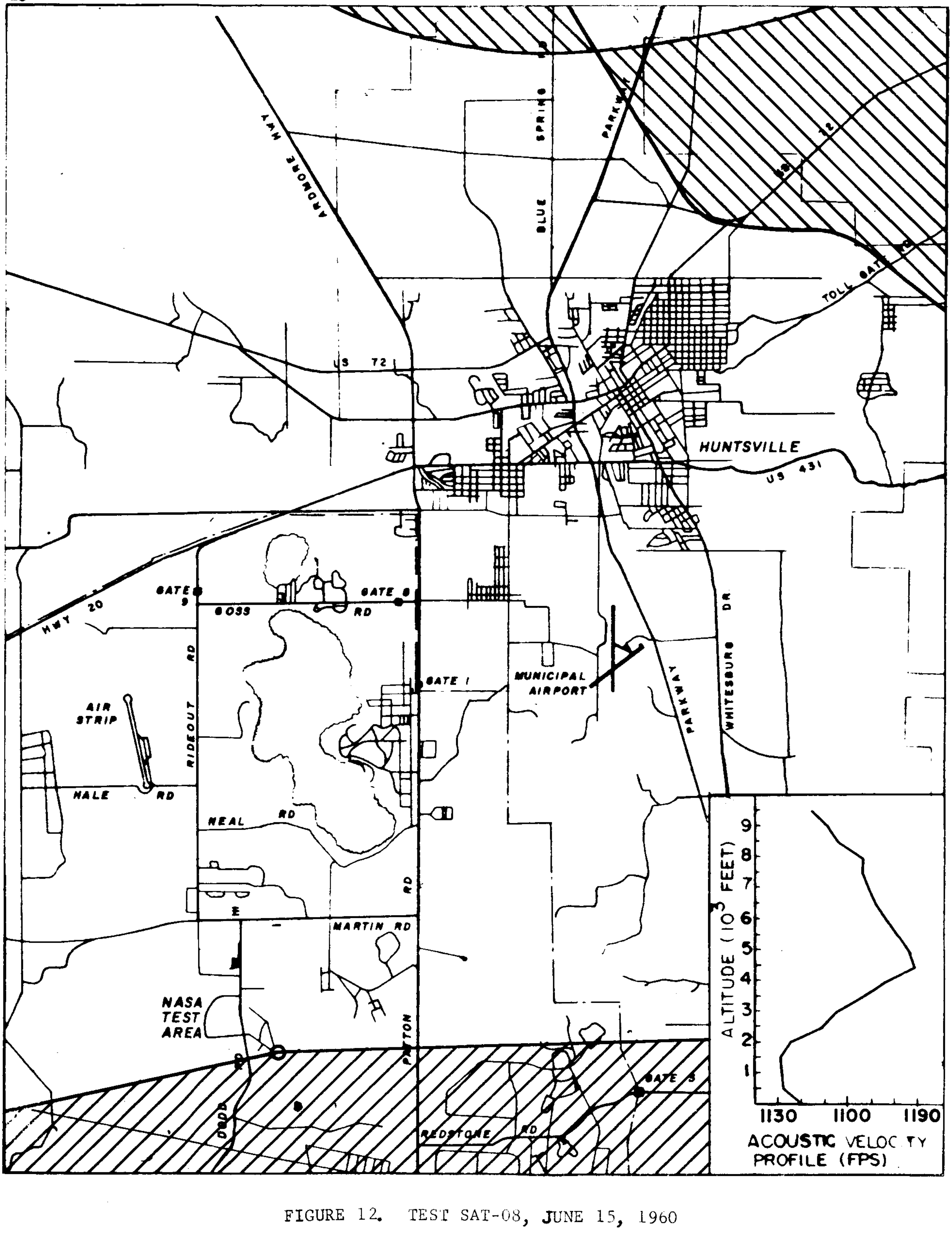

FIGURE 12. TEST SAT-08, JUNE 15, 1960

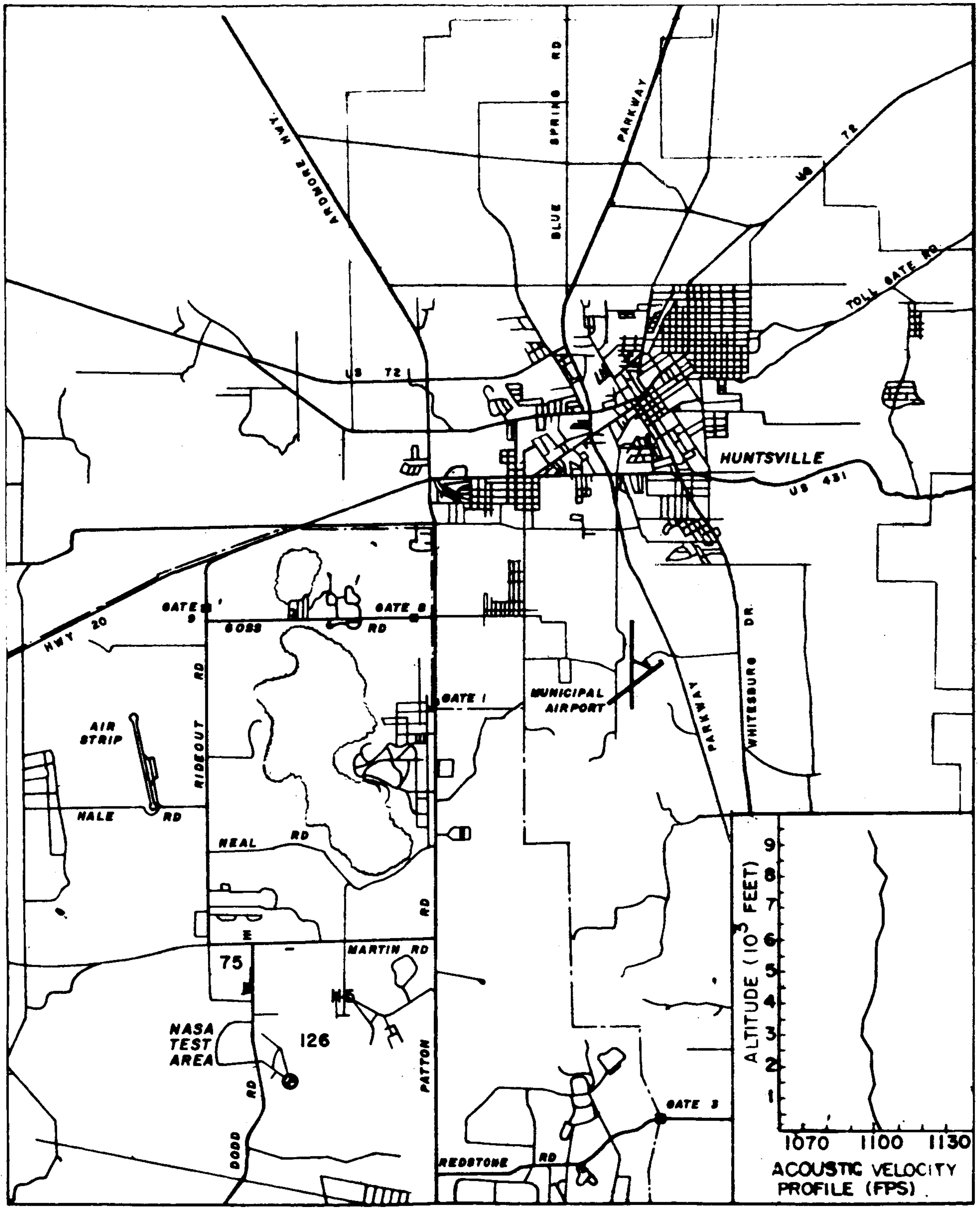

FIGURE 13. TEST SAT-09, DECEMBER 2, 1960

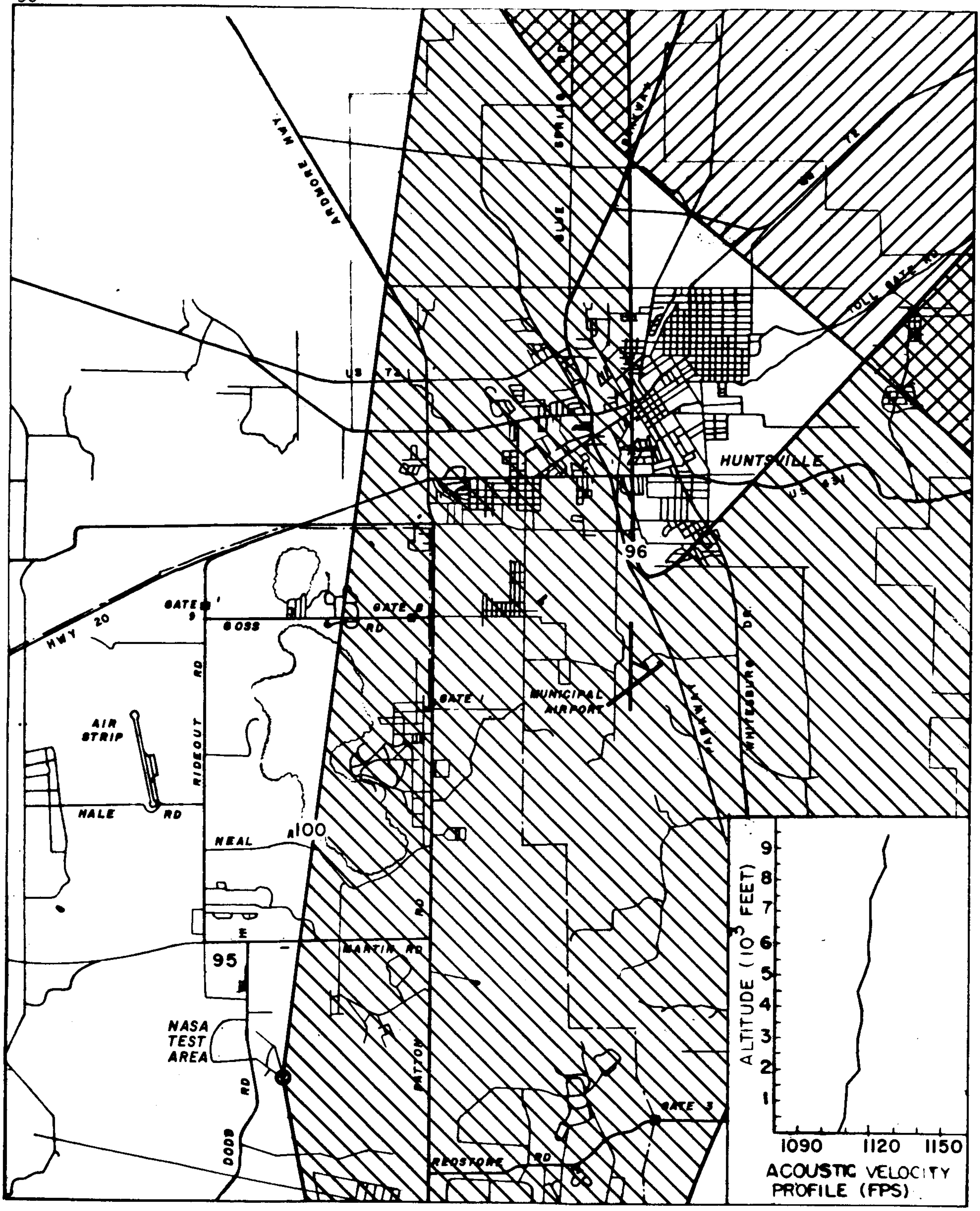

FIGURE 14. TEST SAT-10, DECEMBER 10, 1960

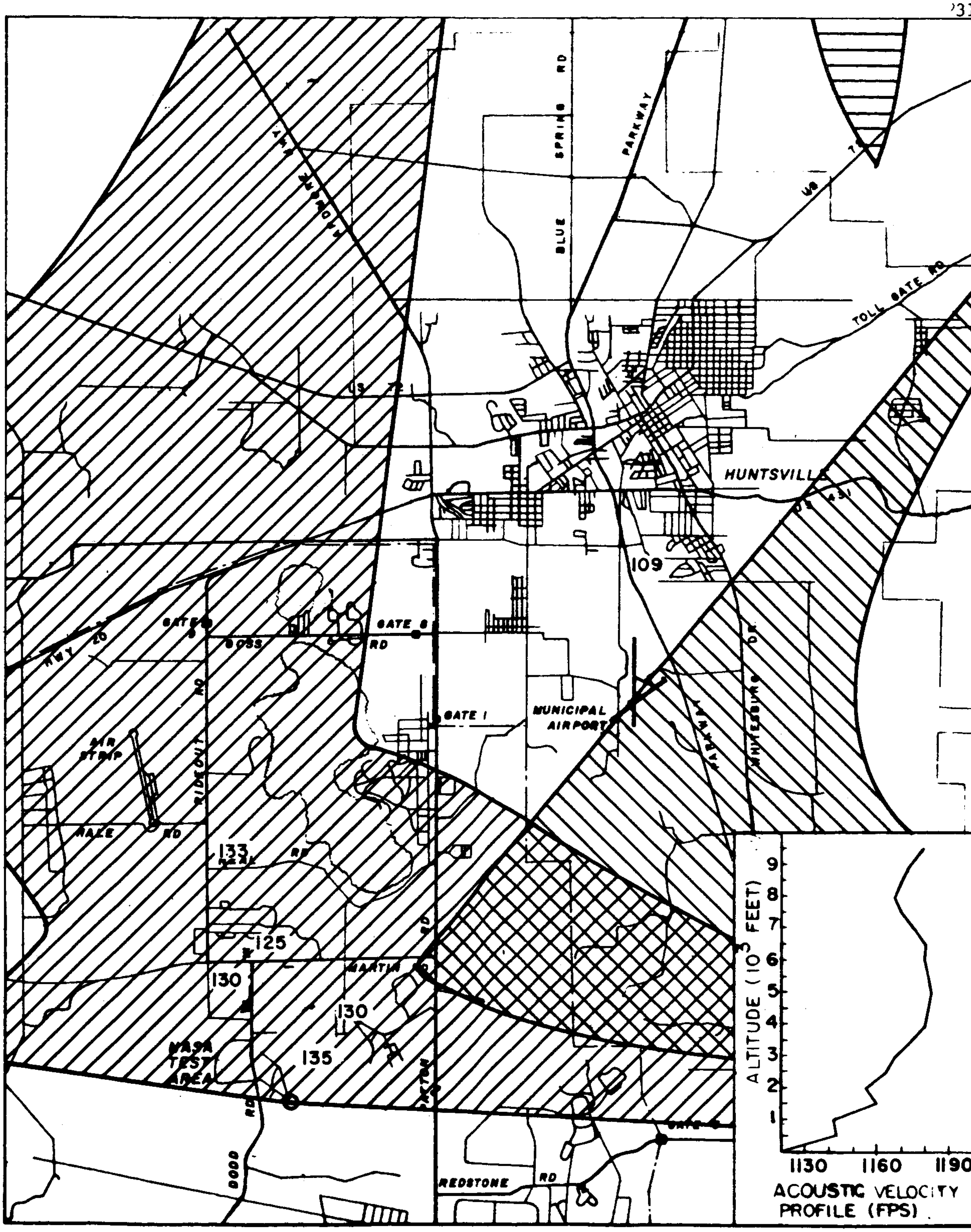

FIGURE 15. TEST SAT-11, DECEMBER 20, 1960

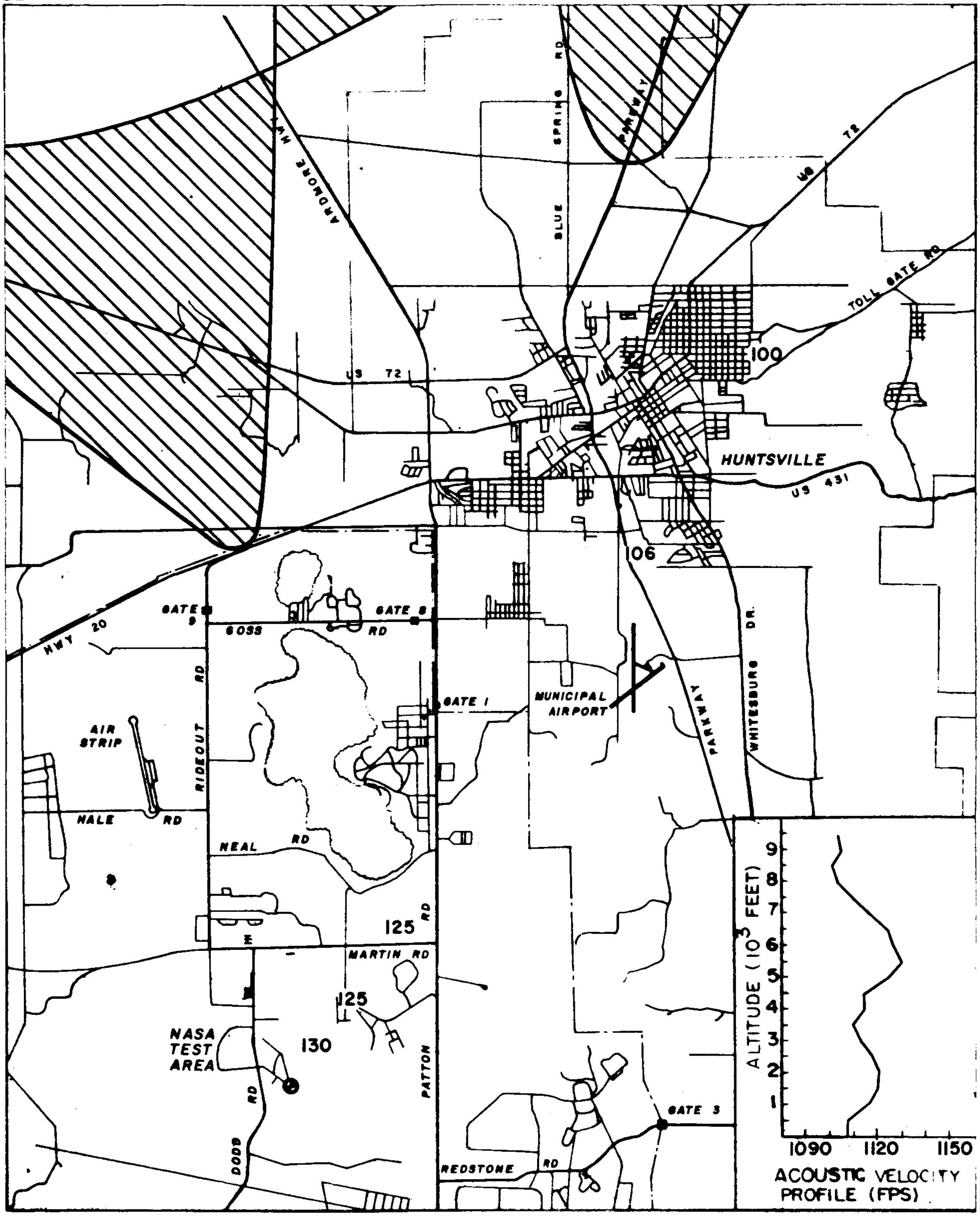

FIGURE 16. TEST SAT-12, JANUARY 31, 1961

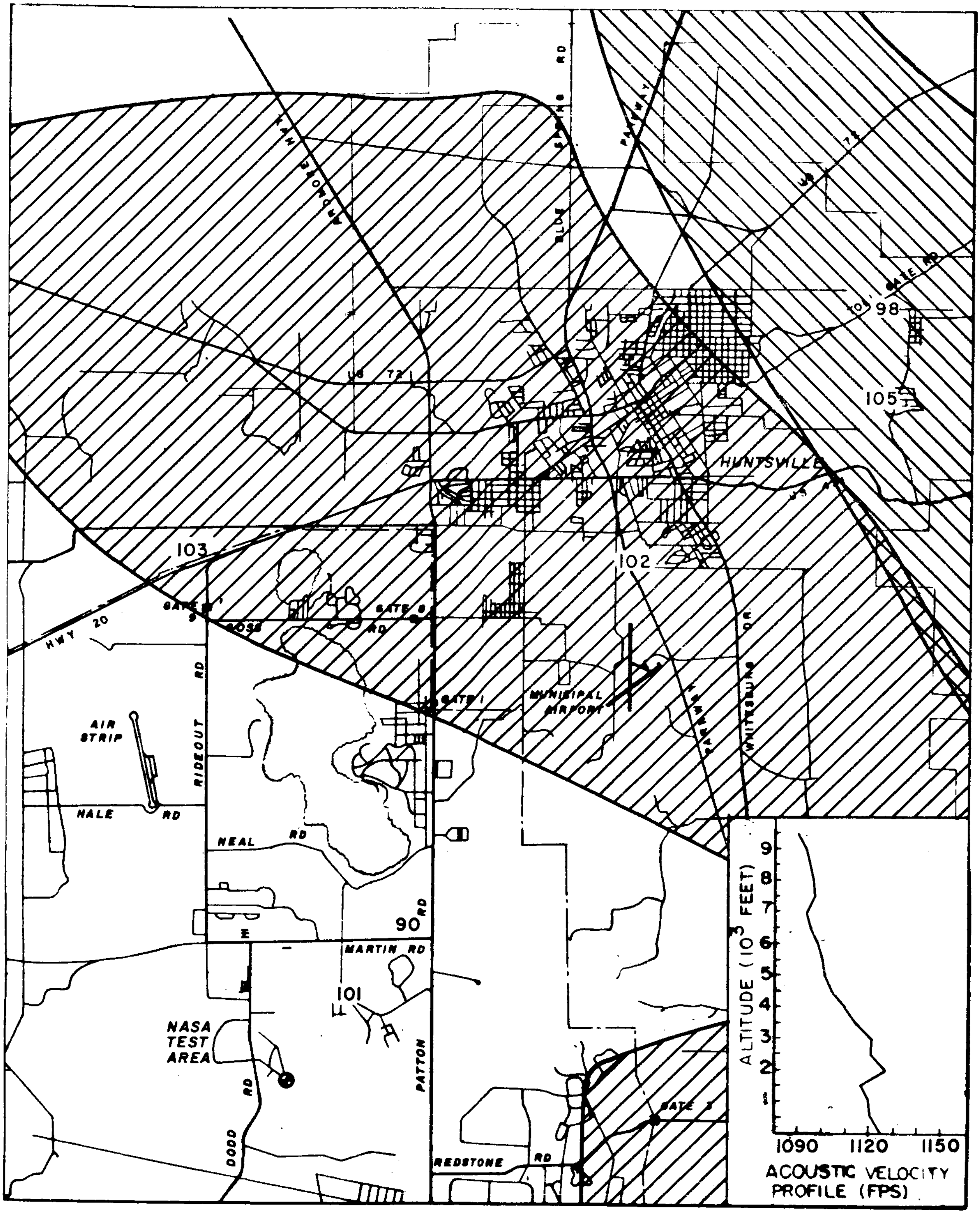

FIGURE 17. TEST SAT-13, FEBRUARY 14, 1961

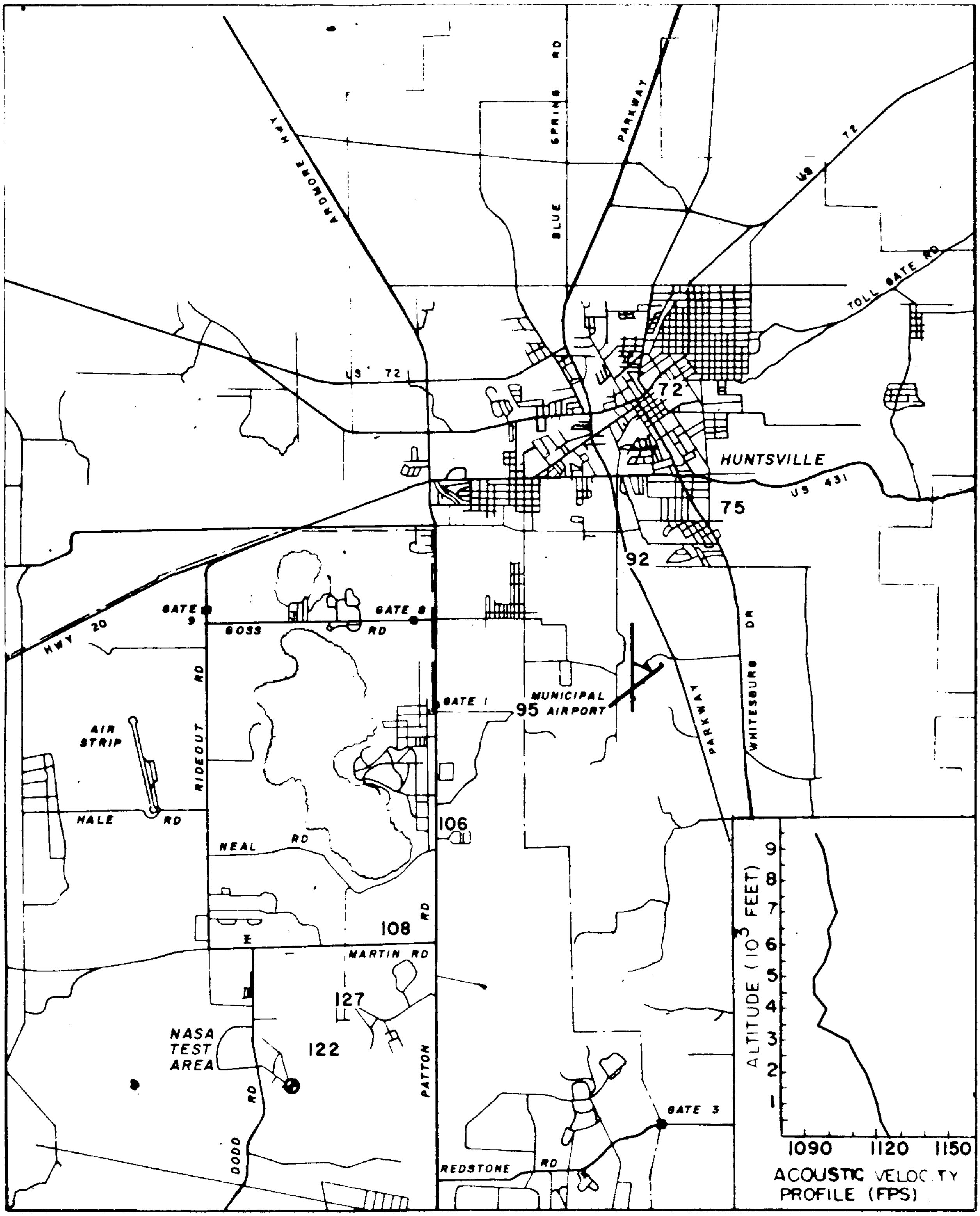

FIGURE 18. TEST SA-01, APRIL 29, 1961

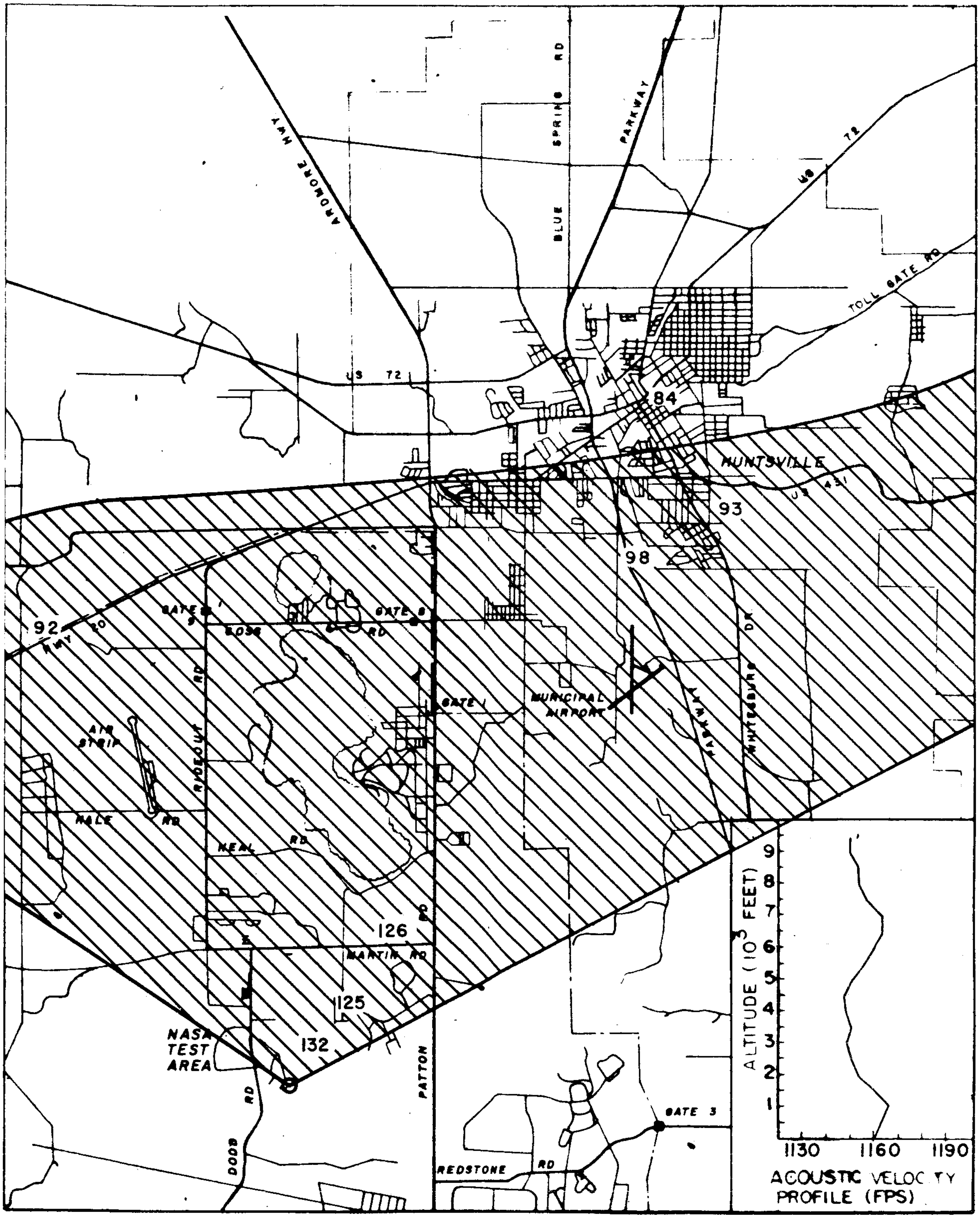

FIGURE 19. TEST SA-02, MAY 5, 1961

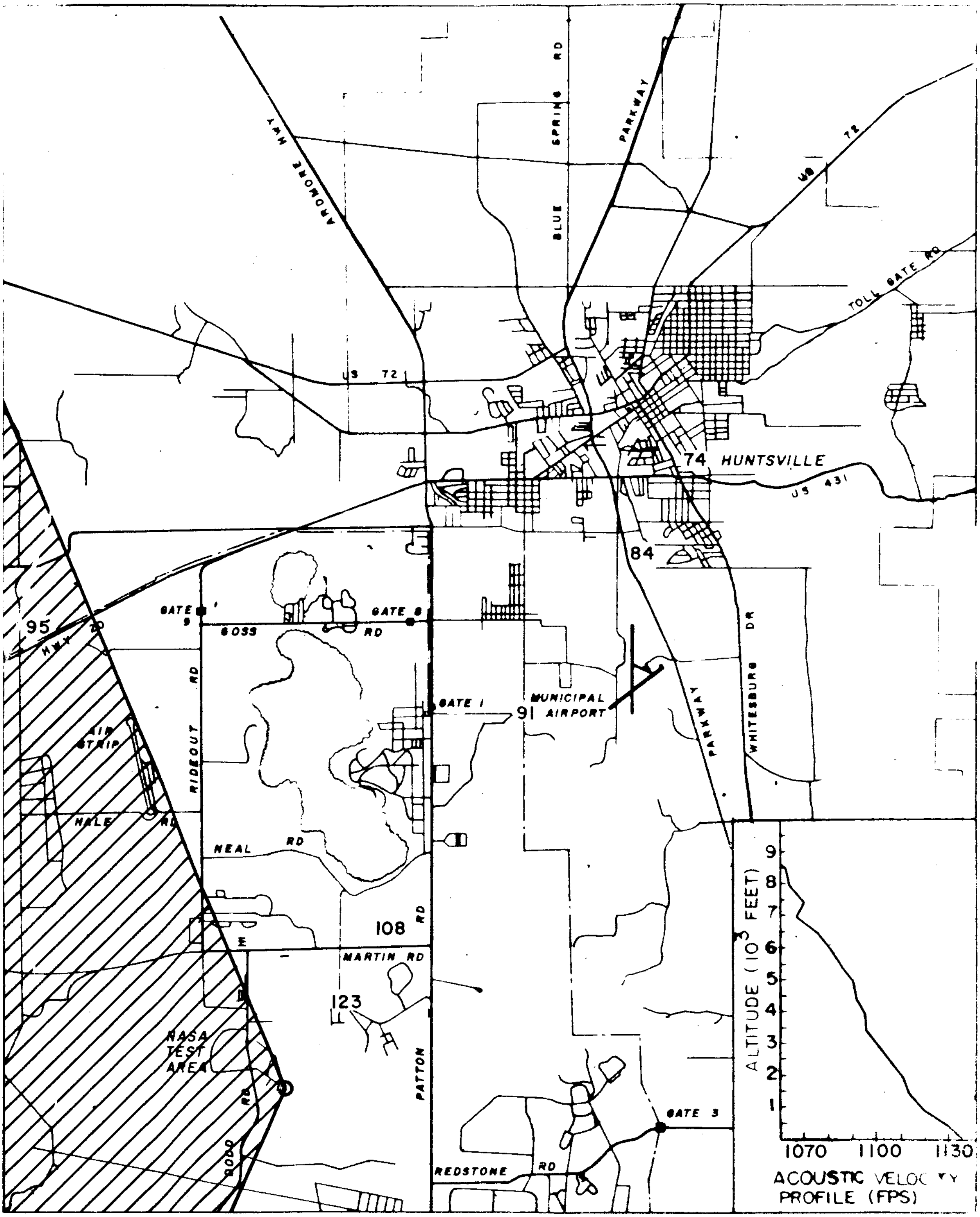

FIGURE 20. TEST SA-03, MAY 11, 1961

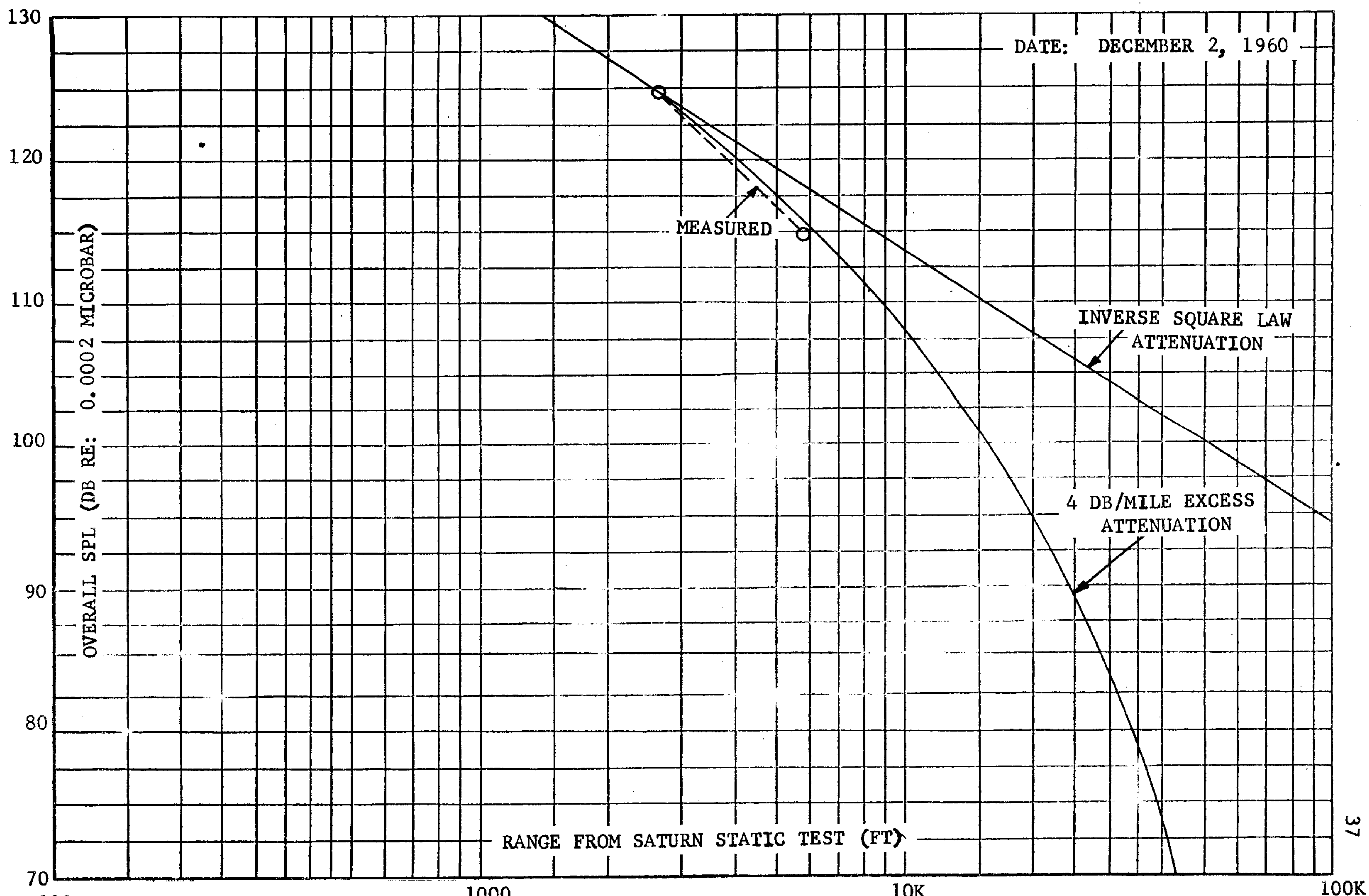

FIGURE 21. OVERALL SOUND PRESSURE LEVELS AT VARIOUS RANGES FROM SATURN TEST SAT-09

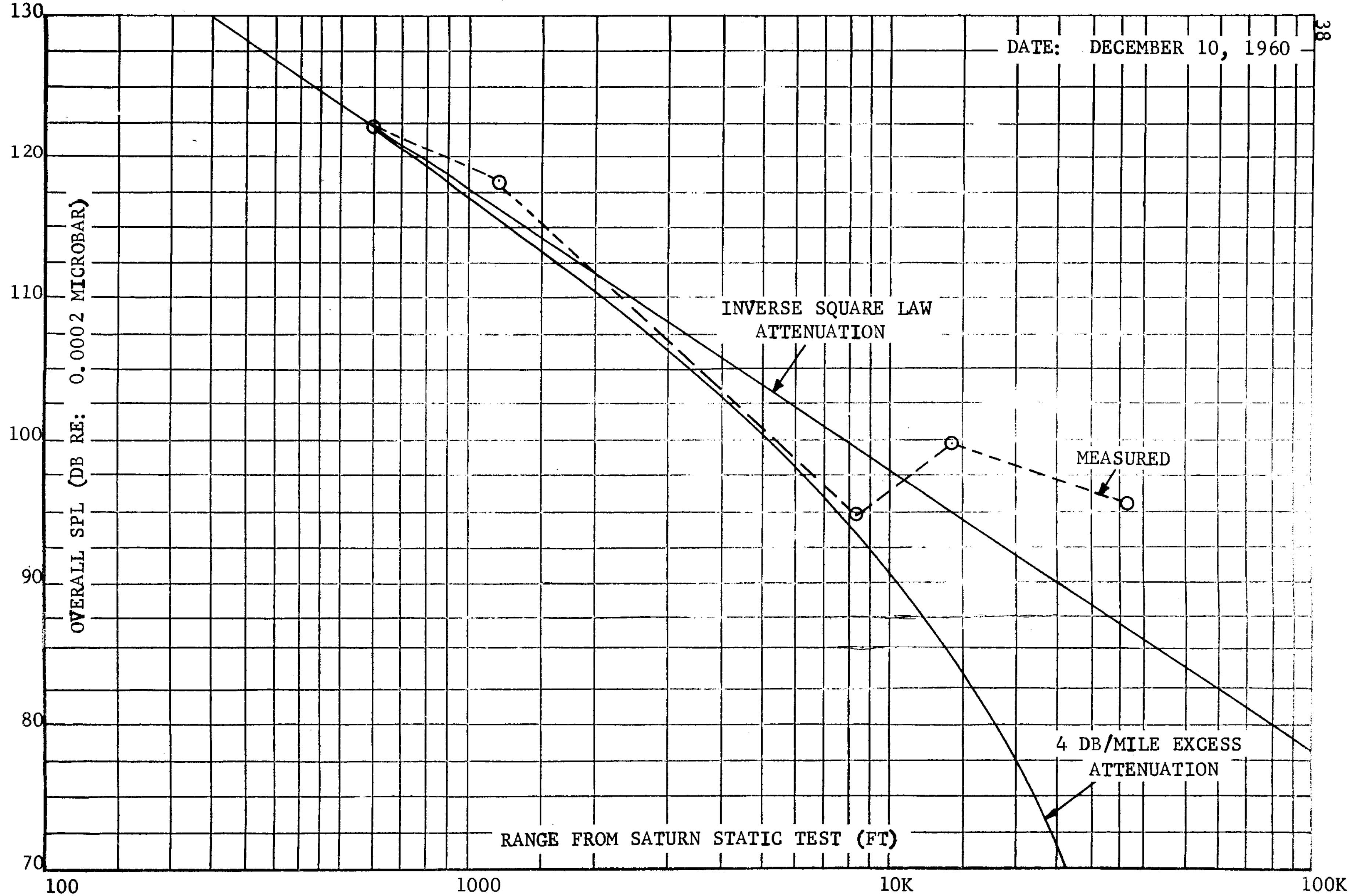

FIGURE 22. OVERALL SOUND PRESSURE LEVELS AT VARIOUS RANGES FROM SATURN TEST SAT-10

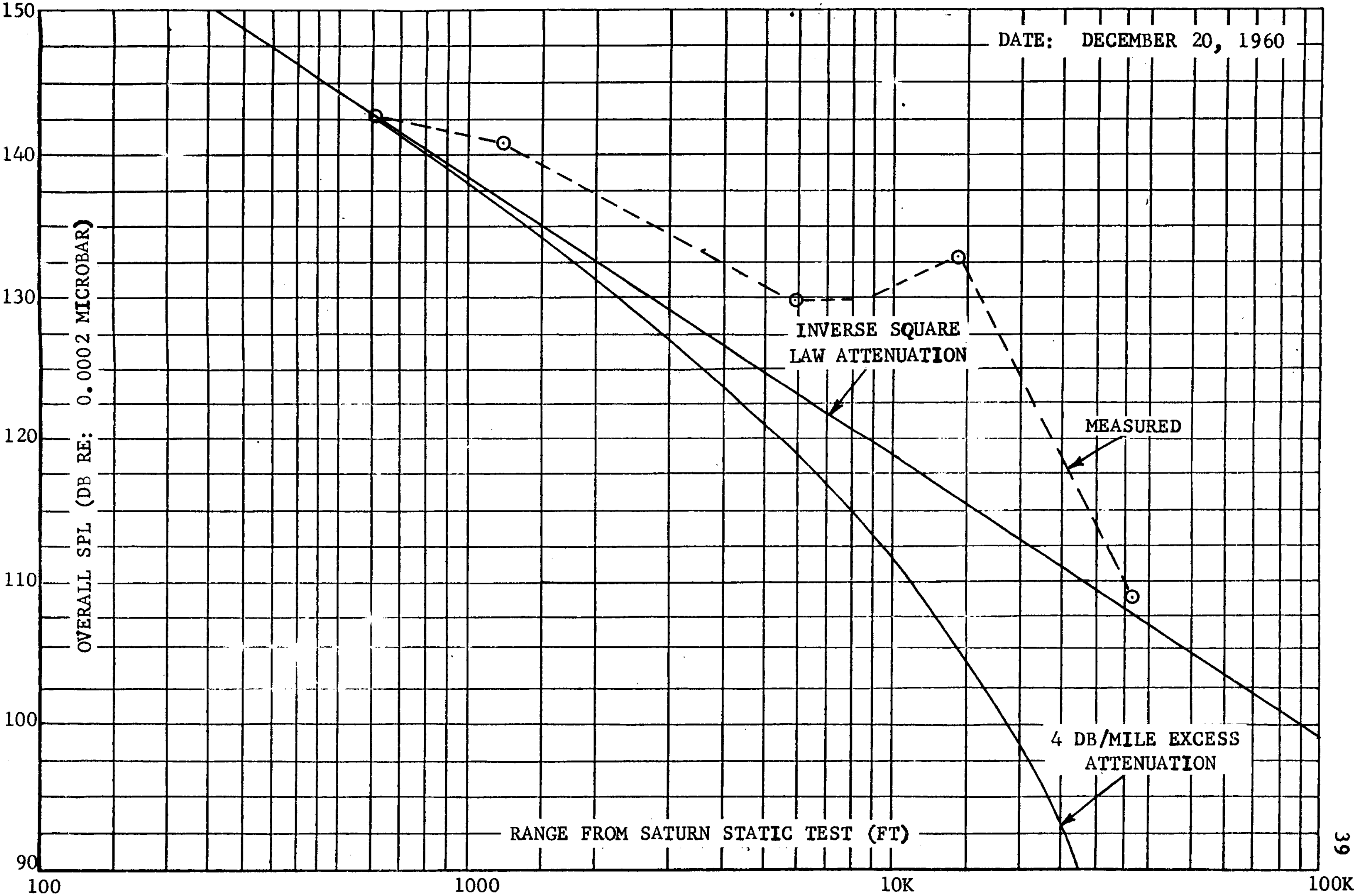

FIGURE 23. OVERALL SOUND PRESSURE LEVELS AT VARIOUS RANGES FROM SATURN TEST SAT-11

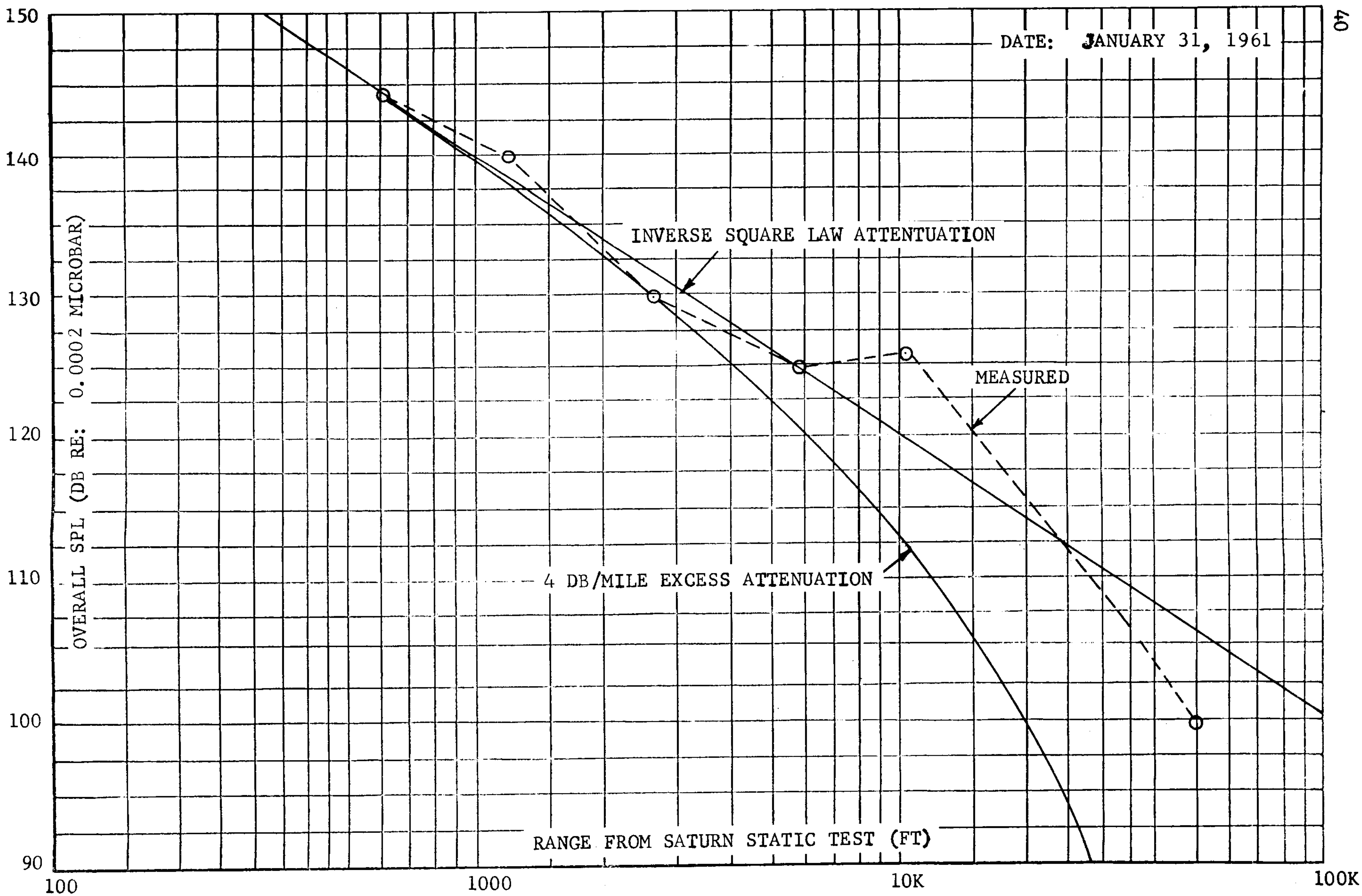

FIGURE 24. OVERALL SOUND PRESSURE LEVELS AT VARIOUS RANGES FROM SATURN TEST SAT-12

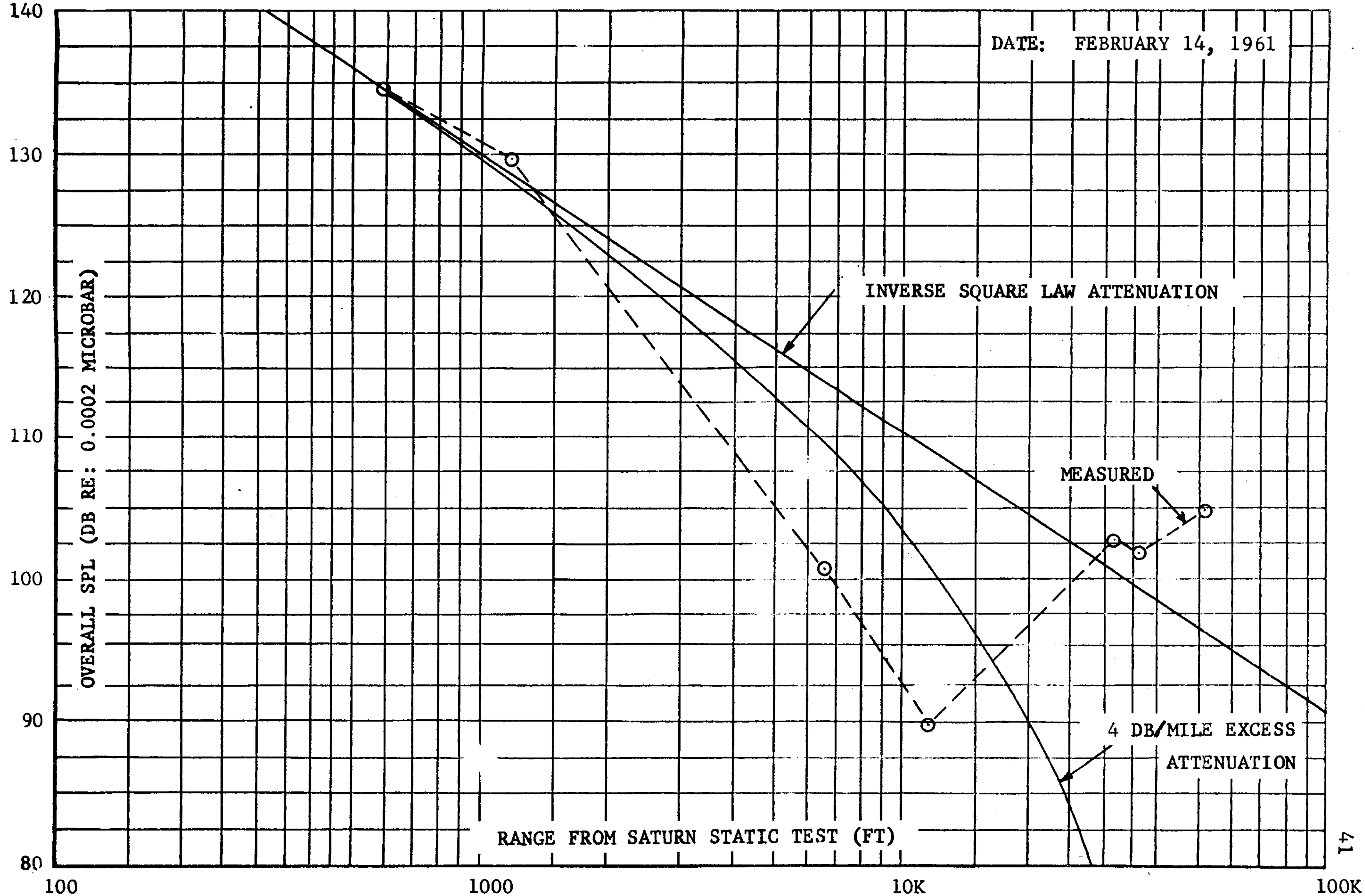

FIGURE 25. OVERALL SOUND PRESSURE LEVELS AT VARIOUS RANGES FROM SATURN TEST SAT-13

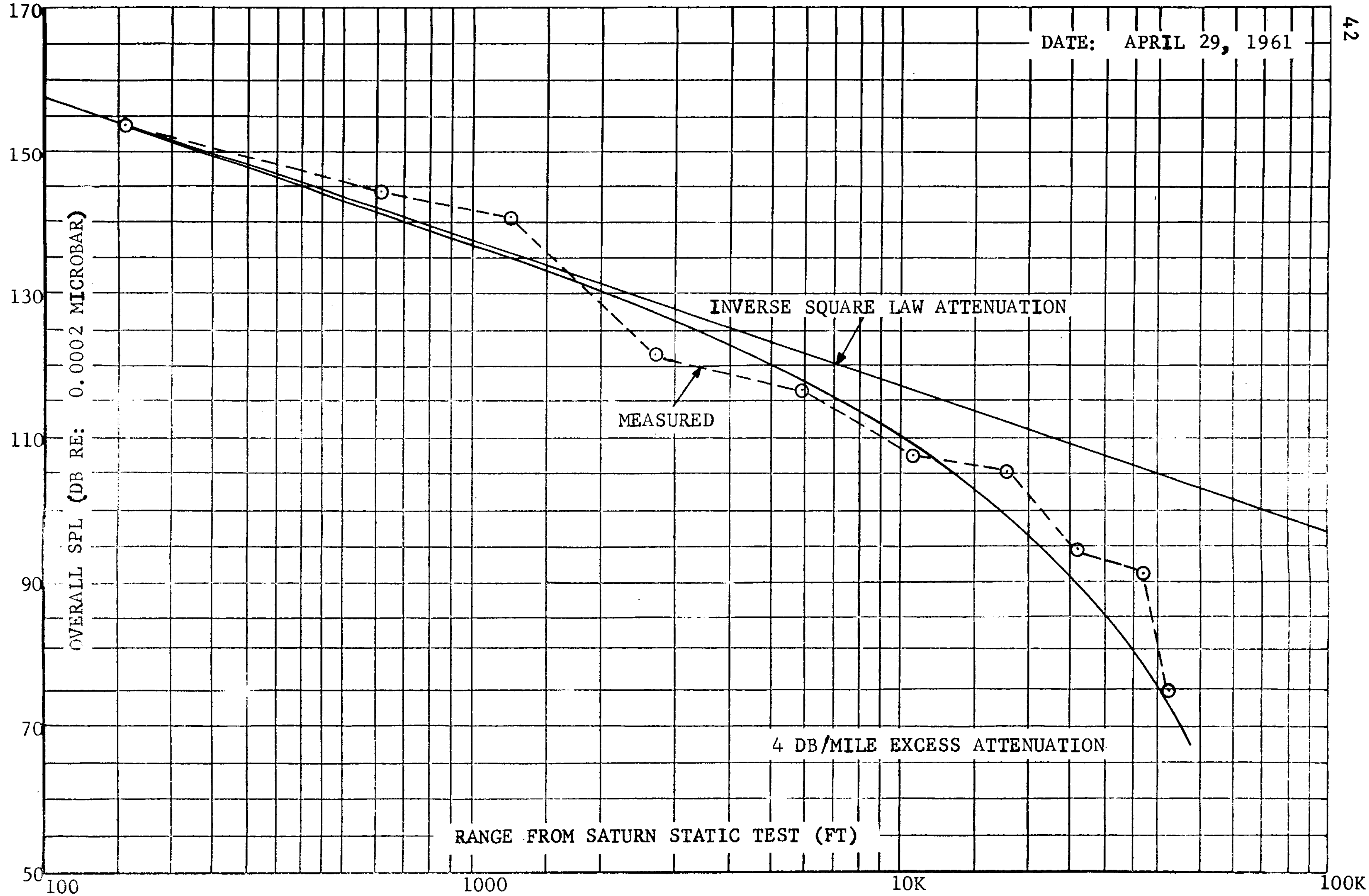

FIGURE 26. OVERALL SOUND PRESSURE LEVELS AT VARIOUS RANGES FROM SATURN TEST SA-01

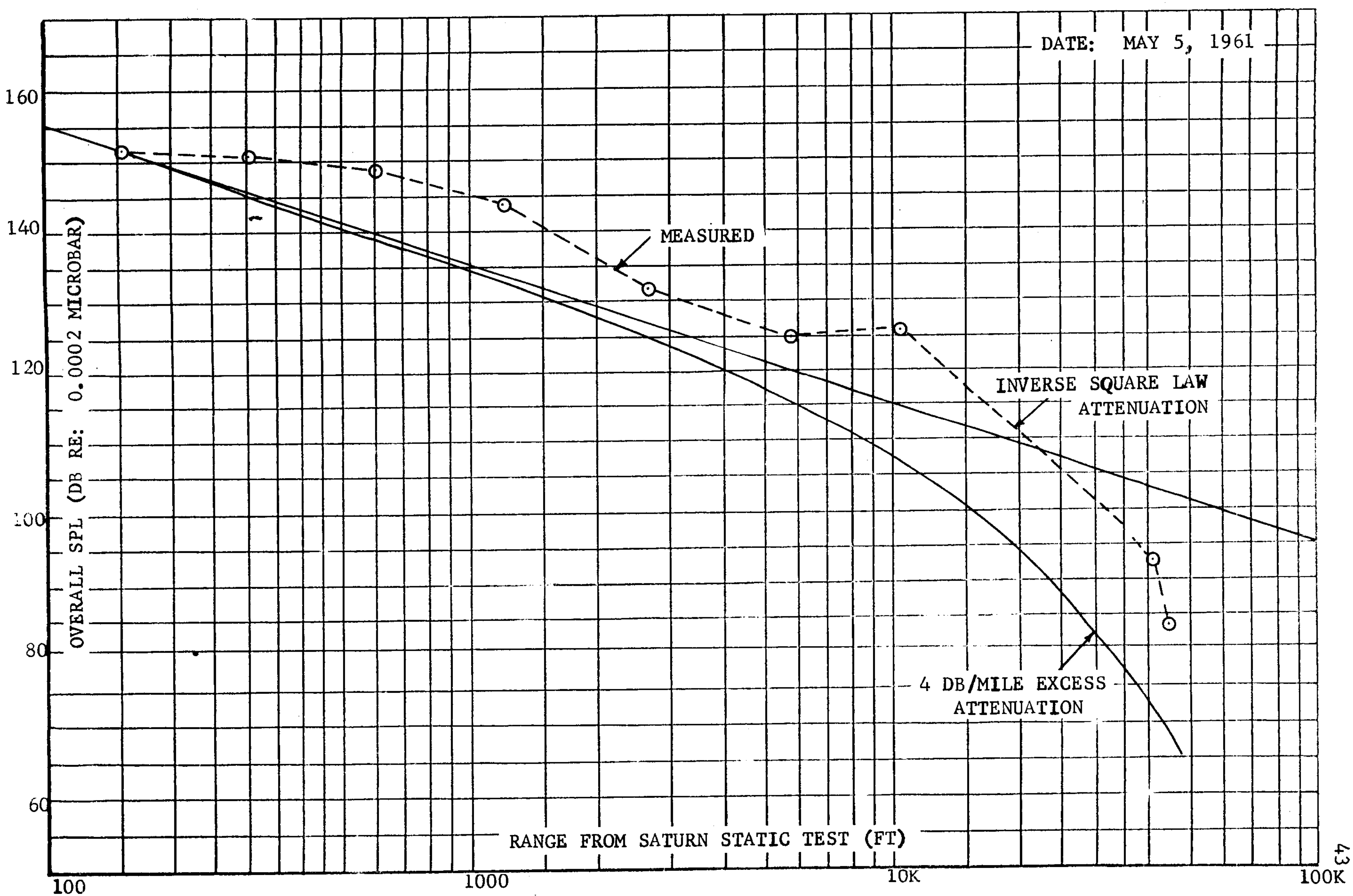

FIGURE 27. OVERALL SOUND PRESSURE LEVELS AT VARIOUS RANGES FROM SATURN TEST SA-02

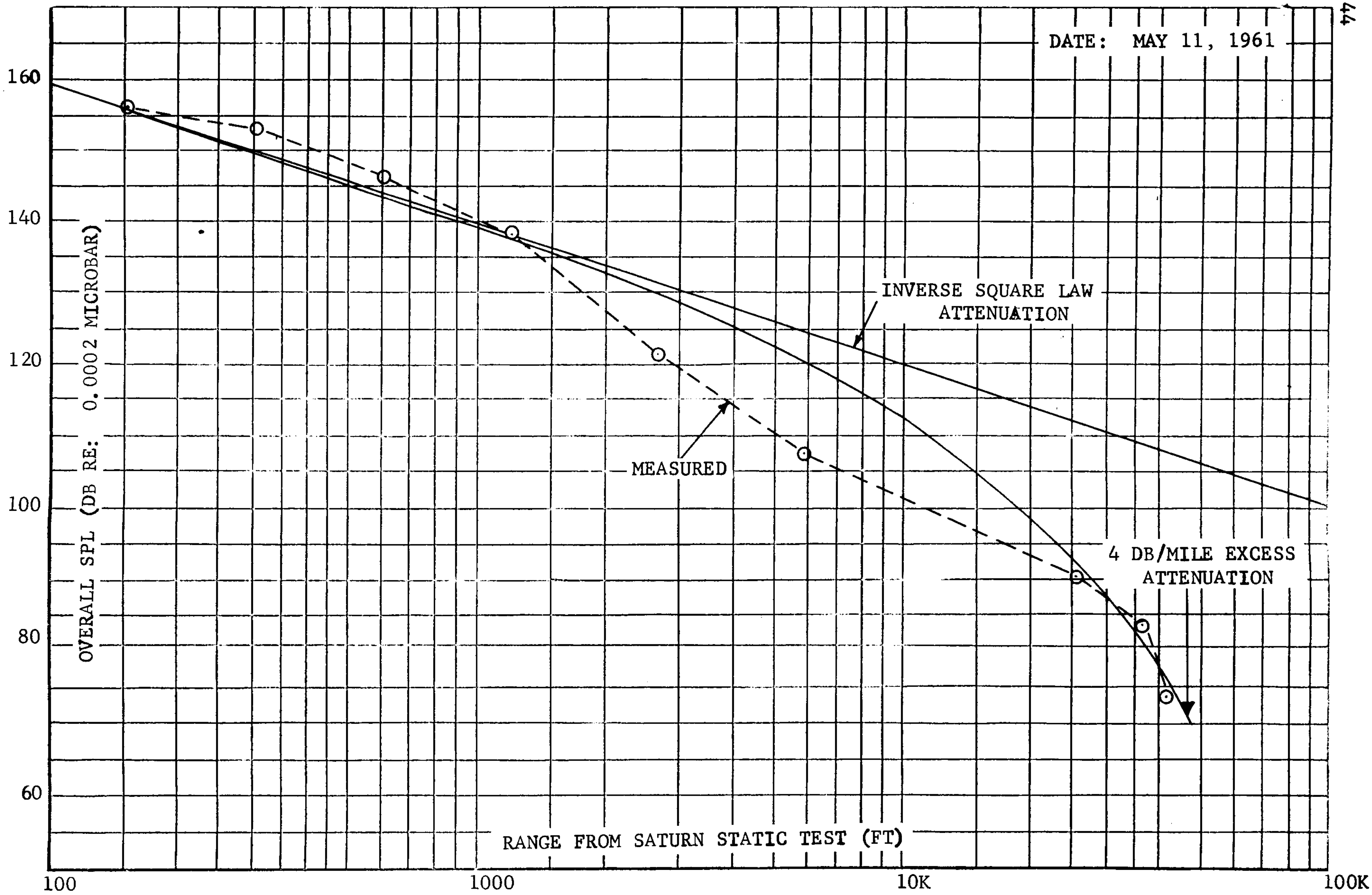

FIGURE 28. OVERALL SOUND PRESSURE LEVELS AT VARIOUS RANGES FROM SATURN TEST SA-03

REFERENCES

1. Perkins, Beauregard Jr., et al, "Forecasting the Focus of Air Blasts Due to Meteorological Conditions in the Lower Atmosphere", BRL Report 1118, Aberdeen Proving Ground, October 1960.

2. Cox, Everett F., et al, "Meteorology Directs Where Blast Will Strike", Bull of American Meteorology Society, Vol. 35, pp 95-103, 1954.

3. Barnes, Thomas G., "Velocity Gradient Method of Ray Tracing in the Atmosphere", Schellenger Research Foundation, August 1956.

4. Dean, E. Allen, "Absorption of Low Frequency Sound in a Homogeneous Atmosphere", Schellenger Research Foundation, August 1959.

5. Davis, Hallowell, et al, "Noise and the Community", Armed Forces - National Research Council Committee on Hearing and Bio-Acoustics, CHABA Report No. 4, October 1954.

6. Mayes, William H., et al, "Near-Field and Far-Field Noise Surveys for a Range of Nozzle Exit Pressures", NASA-Langley Research Center, Technical Note D-21, August 1959.

7. Benson, R. W. and Karplus, H. B., "Sound Propagation Near the Earth's Surface as Influenced by Weather Conditions", Armour Research Foundation, March 1958.

8. Beranek, Leo L., "Acoustic Measurements" John Wiley & Sons, New York, pp 64-83, 1949.

9. Mitchell, Robert P., "Notes on the Theory of Longitudinal Wave Motion in the Atmosphere", White Sands Signal Corps Agency, Meteorological Report No. 1-56, February 1956.

10. Mintzer, David, "Wave Propagation in a Randomly Inhomogeneous Medium", Physics Dept., Brown University, September 1953.

Acoustic Focal Zones Around Saturn Static Tests
APPROVALS

C. C. Thornton

C. C. Thornton
Chief, Special Projects Unit
Component Instrumentation Section

Karl L. Heimburg

Karl L. Heimburg
Director, Test Division

DISTRIBUTION

M-DIR

M-DEP-R&D

M-PIO (2)

M-SAT (2)

M-FUT

M-AERO-DIR

M-AERO-TS

M-AERO-G (2)

M-P&VE-S (3)

M-LOD-DIR

M-LOD-P

M-LOD-T (2)

M-LOD-D (2)

M-LOD-GE (2)

M-LOD-SA

M-LOD-SAI

M-LOD-SP

M-TEST-DIR (2)

M-TEST-TS

M-TEST-PC

M-TEST-M (2)

M-TEST-MC (100)

M-MS-IP

M-MS-IPL (8)

M-MS-H

M-PAT
Mr. John Warden